CD31+ Extracellular Vesicles from Patients with Type 2 Diabetes Shuttle a miRNA Signature Associated with Cardiovascular Complications

03 January 2025

CD31 Positive-Extracellular Vesicles from Patients with Type 2 Diabetes Shuttle a miRNA Signature Associated with Cardiovascular Complications

Francesco Prattichizzo[+*1], Valeria De Nigris[+2], Jacopo Sabbatinelli*[3], Angelica Giuliani[3], Carlos Castaño[2,4], Marcelina Párrizas[2,4], Isabel Crespo[5], Annalisa Grimaldi[6], Nicolò Baranzini[6], Rosangela Spiga[7], Elettra Mancuso[7], Maria Rita Rippo[3], Antonio Domenico Procopio[3,8], Anna Novials[2,4], Anna Rita Bonfigli[9], Silvia Garavelli[10], Lucia La Sala[1], Giuseppe Matarese[10,11], Paola de Candia[1], Fabiola Olivieri[3,8], Antonio Ceriello[1]

1- IRCCS MultiMedica, Milan, Italy
2- Institut d'Investigacions Biomèdiques August Pi i Sunyer (IDIBAPS), Barcelona, Spain
3- Department of Clinical and Molecular Sciences, DISCLIMO, Università Politecnica delle Marche, Ancona, Italy
4- Spanish Biomedical Research Center in Diabetes and Associated Metabolic Disorders (CIBERDEM), Barcelona, Spain.
5- Cytometry and Cell Sorting Facility, CEK, IDIBAPS, Barcelona, Spain
6- Department of Biotechnology and Life Sciences, University of Insubria, Varese, Italy
7- Department of Medical and Surgical Sciences, University "Magna Graecia" of Catanzaro, Catanzaro, Italy
8- Centre of Clinical Pathology and Innovative Therapy, IRCCS INRCA, Ancona, Italy
9- Scientific Direction, IRCCS INRCA, National Institute, Ancona, Italy
10- Istituto per l'Endocrinologia e l'Oncologia Sperimentale "G. Salvatore", Consiglio Nazionale delle Ricerche, Naples, Italy.
11- Department of Molecular Medicine and Medical Biotechnology, University of Naples 'Federico II', via Pansini 5, 80131 Naples, Italy

+ These authors contributed equally to the work

***Corresponding authors**

Francesco Prattichizzo, PhD
IRCCS MultiMedica
Via Fantoli 16/15 Milano, Italy
francesco.prattichizzo@multimedica.it

Jacopo Sabbatinelli, MD, PhD
Department of Clinical and Molecular Sciences, DISCLIMO, Università Politecnica delle Marche,

Diabetes Publish Ahead of Print, published online October 23, 2020

33 Via Tronto, 10/a Ancona, Italy

34 j.sabbatinelli@pm.univpm.it

35
36

ABSTRACT

Innovative biomarkers are needed to improve the management of patients with type 2 diabetes mellitus (T2DM). Blood circulating miRNAs have been proposed as a potential tool to detect T2DM complications but the lack of tissue specificity, among other reasons, has hampered their translation to clinical settings. Extracellular vesicle (EV)-shuttled miRNAs have been proposed as an alternative approach. Here, we adapted an immunomagnetic bead-based method to isolate plasma CD31 positive ($^+$) EVs to harvest vesicles deriving from tissues relevant for T2DM complications. Surface marker characterization showed that CD31$^+$ EVs were also positive for a range of markers typical of both platelets and activated endothelial cells. After characterization, we quantified 11 candidate miRNAs associated with vascular performance and shuttled by CD31$^+$EVs in a large (n=218), cross-sectional cohort of patients categorized as T2DM without complications, T2DM with complications, and controls. We found that 10 of the tested miRNAs are affected by T2DM, while the signature composed by miR-146a, -320a, -422a, -451a efficiently identified T2DM patients with complications. Furthermore, another CD31$^+$EV-shuttled miRNA signature, i.e. miR-155, -320a, -342-3p, -376, and -422a, detected T2DM patients with a previous major adverse cardiovascular event. Many of these miRNAs significantly correlate with clinical variables held to play a key role in the development of complications. In addition, we show that CD31$^+$ EVs from patients with T2DM are able to promote the expression of selected inflammatory mRNAs, *i.e. CCL2*, *IL-1α*, and *TNFα*, when administered to endothelial cells *in vitro*. Overall, these data suggest that the miRNA cargo of plasma CD31$^+$ EVs is largely affected by T2DM and related complications, encouraging further research to explore the diagnostic potential and the functional role of these alterations.

Keywords: extracellular vesicles; exosomes; CD31; microRNA; type 2 diabetes mellitus; T2DM complications; cardiovascular diseases; MACE; low-grade inflammation.

INTRODUCTION

Type 2 diabetes mellitus (T2DM) is a chronic, heterogeneous disease caused by a multi-layer interaction between the genetic makeup and environmental/lifestyle dependent factors (1). T2DM is the cause of morbidity and mortality, mainly due to its cardiovascular (CV) complications, *e.g.* ischemic heart disease and peripheral vascular disease (2). A number of additional alterations concur to the development of CV complications in diabetic patients (1; 3). Given the complexity and heterogeneity of the disease, many potential biomarkers for the development of CV diseases in T2DM patients have been explored (4).

Blood circulating miRNAs have been proposed as a potential tool to improve CV risk assessment among patients with T2DM and other conditions (5-7). Given plasma miRNA stability and their ability to sense environmental stressors and modulate multiple pathways accordingly, miRNAs seem to be the ideal candidates to provide useful information in complex and heterogeneous diseases like T2DM complications and CV diseases in general (8; 9). However, at present, neither single miRNAs nor miRNA signatures have been translated into clinical settings for diagnostic purposes. Many reasons have hampered their use as biomarkers, including the lack of disease specificity and the confounding effect provided by the relative contributions of different tissues to the plasma miRNA pool (10; 11). To overcome these issues, the isolation of specific miRNA cargos, and in particular of extracellular vesicles (EV)s, has been proposed (10; 12).

EVs are membrane-coated nanoparticles actively and/or passively released by almost all cell types. EVs can be categorized according to a specific characteristic or by their size. Small EVs (diameter <100 nanometres) derive from either multivesicular bodies or the plasma membrane, while larger vesicles (between 100 nanometres and 1 micron) mostly derive from the plasma membrane (13). Both EV types are able to shuttle and deliver functional nucleic acids, including miRNAs. Blood contains a heterogeneous mixture of EVs of different origin, which are currently being characterized for therapeutic and diagnostic purposes (14-16). In particular, recent evidence suggests a key role for EV-shuttled miRNAs in the etiopathogenesis of both T2DM and its vascular complications (17-20).

However, few studies have quantified the miRNA payload of circulating EVs in relation to human T2DM (21; 22), while only one study assessed EV-shuttled miRNAs in a setting of T2DM complications (23). A recent paper showed that the majority of circulating EV-shuttled miRNAs derive from the adipose tissue, a key organ for the development of T2DM (24). On the other side, platelets, immune cells, and endothelial cells play a prominent role in the development of T2DM-related complications (25; 26). Given the marked and specific expression of CD31, *i.e.* platelet endothelial cell adhesion molecule (PECAM-1), in these three cell types, we adapted a previously published immunomagnetic method (27) using commercially available beads to selectively capture CD31 positive (+) EVs from plasma. After MISEV guidelines-driven characterization, we measured a panel of 11 miRNAs previously associated with vascular performance in a cross-sectional cohort of 218 subjects, categorized as healthy controls (Ctrl), patients with T2DM but without complications (NC), and T2DM patients with complications (C). Here, we provide the first evidence of a specific miRNA signature shuttled by $CD31^+$EVs able to efficiently discriminate between T2DM patients with complications from those without complications, and show that $CD31^+$ EVs from patients with T2DM are able to promote pro-inflammatory pathways when administered to endothelial cells *in vitro*.

RESEARCH DESIGN AND METHODS

Cohort description, plasma isolation, and sample size

Samples derive from a previously published cohort composed of 501 patients with T2DM and 400 healthy control subjects (28). Informed consent was obtained from each subject and the study protocol was approved by the local research ethics committee. T2DM was diagnosed according to the ADA criteria (29). Inclusion criteria for patients with diabetes were BMI < 40 kg/m^2, age 35–85years, ability and willingness to give written informed consent. Information collected included data on vital signs, anthropometric factors, medical history, and behaviors. The presence/absence of diabetic complications was evidenced as follows: diabetic retinopathy by fundoscopy through dilated pupils

and/or fluorescence angiography; nephropathy, defined as a urinary albumin excretion rate >30mg/24h and/or an estimated glomerular filtration rate (eGFR) <60 ml/min per 1.73m^2; neuropathy established by electromyography; ischemic heart disease defined by clinical history, and/or ischemic electrocardiographic alterations; peripheral vascular disease, including atherosclerosis obliterans and cerebrovascular disease based on history, physical examinations, and Doppler velocimetry. Among the 101 patients analyzed with T2DM and at least one complication, 28 had neuropathy, 22 peripheral vascular disease, 20 nephropathy, 48 retinopathy and 52 major adverse cardiovascular events (MACE). Healthy subjects were selected from a larger population of subjects belonging to a prevention program (30). Concentrations of common analytes were measured by standard procedures. As suggested by the MISEV initiative (65), fasting blood samples (collected in 4ml plasma EDTA tubes) of all subjects were centrifuged at 753 g at 4°C to obtain platelet-poor EDTA plasma and stored at −80°C within 3 hours from blood collection. Sample size was calculated based on our previous publications (9; 31; 32).

Isolation of CD31$^+$ extracellular vesicles

Plasma EDTA samples were allowed to thaw at room temperature. Appropriate volume (100 µl when used for singular miRNA dosage, as indicated in the text for the other experiments) was diluted with an equal amount of PBS. To remove apoptotic bodies and residual cellularity, sample were pre-cleared by two subsequent centrifugations at 4°C, one at 2’000 *g* for 30 minutes and the following at 10’000 *g* for 45 minutes. Supernatant is diluted with PBS to reach 500 µl of volume and then mixed with FcR Blocking Reagent (20 µl) provided in the commercially available kit for endothelial cells isolation (130-091-935, Miltenyi Biotec). After vortexing, 20 µl of CD31 MicroBeads (130-091-935, Miltenyi Biotec) are added to the suspension and incubated at 4° C in the dark for 30 minutes. Appropriate (according to reaction volume) columns are mounted on the magnetic field and activated with PBS. After incubation, the mixture is loaded onto the column to allow separation. After 3 washing with 500 µl of PBS, the column is removed from the magnetic support and CD31$^+$EVs are eluted in 500 µl PBS with the help of a plunger (**Figure 1A**). As a negative control, isotype control

beads (Dynabeads M-280) and no beads (equal amount of PBS) were used for parallel isolation of EVs to test for eventual non-specific bindings of EVs and subjected to MACSPlex comparison (methods below). We have submitted all relevant data of our experiments to the EV-TRACK knowledgebase (EV-TRACK ID: EV200038) (33).

Isolation of extracellular vesicles through ultracentrifugation

For comparative experiments, an aliquot of 1 ml of plasma was pre-cleared as indicated above and then the supernatant was diluted with PBS and subjected to ultracentrifugation at 120'000 *g* (4ºC) in an S110AT rotor in a Sorvall MX 150 ultracentrifuge (Thermo Scientific Inc) for 1,5 hours. Pellets were resuspended in PBS and ultra-centrifuged again at 120'000 *g* for an additional 1,5 hours. The final pellets were resuspended in 500 µl of PBS. In one case, the depleted fraction of the CD31 isolation method was collected and subjected to the same steps of ultracentrifugation to undergo nanoparticle tracking analysis.

Nanoparticle tracking analysis (NTA)

$CD31^+$EVs were isolated starting from 1 ml of plasma as described and resuspended in PBS. Size and concentration of vesicles was determined using NanoSight LM10 equipment (Malvern Instruments Ltd) using different dilutions (34) and with the following parameters: camera at 30 frames per second, camera level at 16, temperature between 21–25 °C and video recording time 60 s. Three videos were recorded for each sample and analyzed with NanoSight NTA 3.1 software. Data were expressed as mean ± SD of the three videos.

Transmission electron microscopy (TEM)

To explore vesicles morphology with TEM, 30µl of $CD31^+$EVs samples were diluted with PBS, allowed to dry on top of Formvar carbon coated grids for 25min and contrasted with 2% uranyl acetate for 2min. Preparations were observed in a JEOL 1010 100kV Electron Microscope.

Western Blot

For Western Blot experiments, $CD31^+$ EVs were ultracentrifuged to allow PBS discharge and direct application of lysis buffer to the EV pellet. The same was done with EVs isolated through

ultracentrifuge. EV lysates were prepared in RIPA buffer containing a protease inhibitor cocktail and quantified using the Bradford method. Next, the lysates were subjected to SDS-PAGE and transferred to nitrocellulose membranes (Whatman). Membranes were then incubated with the primary antibodies overnight at 4°C. The following primary antibodies were used: CD31 (#3528, Cell Signaling), Alix (#92880, Cell Signaling), TSG101 (ab125011, Abcam), CD63 (ab59479, Abcam), ApoB100 (ab20737, Abcam), and ApoA1 (sc-30089, Santa Cruz Biotechnology). Fifty μg of whole plasma proteins were also run as positive control for ApoA1. After incubation with the specific HRP-conjugated antibody (Vector), proteins were detected by using enhanced chemiluminescence (ECL) (GE Healthcare) and band densities were quantified by densitometry using ImageJ software.

Cytofluorimetric detection of EV markers

A commercially available (130-108-813, MACSPlex Exosome Kit, Miltenyi) and previously validated (35) kit was used for cytofluorimetric detection of a large range of markers in isolated EVs. Briefly, EVs isolated starting from the same amount of plasma were prepared as described in the manufacturer protocol. The multiplex bead-based platform was analyzed by flow cytometry using a BD FACSCantoII flow cytometer with the corresponding software (Becton, Dickinson and Company, New Jersey, USA) equipped with a 488nm and a 640nm laser. Fluorescence emission was collected by 530/30 nm, 585/42 nm, and 660/20 nm bandpass filters. At least 1’000 beads per sample were examined and mean fluorescence intensity (MFI) was determined using BD FACSDiva 6.1 software. Background signals were determined by analyzing beads incubated only with the respective staining antibodies and subtracted from the signals obtained for beads incubated with EVs and stained with the corresponding antibody. The Multiplex bead-based platform includes Setup Beads for flow cytometer setup.

RNA extraction and miRNA profiling

Plasma samples from 4 subjects were pooled to reach 1 ml. $CD31^{+}$EVs were isolated from 5 Ctrl preparations and 5 T2DM preparations. RNA was extracted with a commercial kit known to enrich small RNA species (Norgen Biotek Corporation). The same amount of RNA was converted to cDNA

by priming with a mixture of looped primers using the manufacturer's instructions (MegaPlex kit, Applied Biosystem). Nine µl of cDNA were used for mature miRNA profiling by a real-time PCR instrument equipped with a 384-well reaction plate and human miRNA Array pool A containing 367 different human miRNA assays in addition to selected small nucleolar RNAs and negative controls (non-human miRNAs). Only miRNAs expressed in more than one sample were included in the analysis. 2^{-Ct} of the average values of each miRNA were used to build the heatmap comparing Ctrl and T2DM with the ClustVis web tool (https://biit.cs.ut.ee/clustvis/) (36). Profiling raw data were deposited in GEO and are accessible with the accession number GSE142553.

Single miRNA quantitation

For single miRNA quantification, $CD31^+$EVs were isolated from 100µl of plasma. After mixing with lysis buffer and before loading to the RNA separation column (Norgen), the synthetic *Caenorhabditis elegans* miRNA, cel-miR-39, was spiked into plasma before RNA extraction. Only samples with cel-miR-39 recovery > 95 % were used in subsequent analyses. Reverse transcription and miRNA amplification were performed as previously described (9). Relative expression corresponded to the $2^{-\Delta Ct}$ value. Given the lack of an adequate endogenous control for plasma circulating miRNAs (11), miRNA expression levels were generally normalized by cel-miR-39 levels, unless indicated otherwise. To validate the 4-miRNA signature as a predictor of MACE in T2DM patients, global mean normalization was performed for each miRNA by subtracting the mean of the Ct values of all the miRNAs assessed in sample *i* from each individual Ct value from sample *i*. To compare the diagnostic performance of $CD31^+$EV-shuttled miRNAs with their whole plasma counterparts, we used previously published data by our group for both miR-146a-5p (32) and miR-21-5p (9), extracting the miRNA quantitation data for the same patients of this study. Previous data were generated using the same amount of plasma, the same quantitation technology, and the same standardization method, thus allowing data comparison through the relative receiver-operating characteristics (ROC) curves as detailed below.

EV fluorescent labelling, loading with cel-miR-39 or fluorescent small RNA, and treatment of endothelial cells

To use $CD31^+$EVs for *in vitro* experiments, these were first detached from beads to avoid non-specific toxicity and allow proper EV delivery to recipient cells. Briefly, EV/beads complexes (in 1.5 ml tubes) were placed on the magnetic stand for 2 minutes. Then, PBS is removed and 300 µl of EXOFLOW buffer (System Biosciences) were added. After incubation on a shaker at 25°C for 2 hours, samples are placed on the magnetic stand to remove the supernatant containing eluted EVs, without disturbing the bead pellet. Collected EVs were quantified using NTA (data not shown).

As *in vitro* model of endothelial cells, human umbilical vein endothelial cells (HUVEC)s were used. HUVECs were cultivated as previously described (38; 39). EV-depleted FBS (through overnight centrifugation) was used for all the experiments. 1 x 10^9 EVs were fluorescently labelled using PKH67 membrane dye (Sigma-Aldrich). Labelled sEVs were washed in 10 ml PBS, collected by ultracentrifugation, resuspended in PBS, and were then incubated with 50'000 recipient HUVECs for 24 h. HUVEC nuclei were counterstained with PBS-diluted 4',6-diamidino-2-phenylindole dihydrochloride (DAPI, Sigma) for 15 minutes and cells were imaged at a widefield microscopy (Axio Observer A1, Zeiss).

HUVECs were also treated for 24 h with EVs transfected with the non-human cel-miR-39 or with a small fluorescent RNA. EVs were transfected with the Exo-Fect kit (System Biosciences) according to the manufacturer's instructions. Briefly, EVs were prepared for transfection by combining Exo-Fect solution, 20 pmol of cel-miR-39 (or the small fluorescent RNA), PBS and 1 x 10^8 EVs. The transfection solution was incubated at 37°C for 10 min and then put on ice. To stop the reaction, the EXoQuick-TC reagent supplied in the kit was added. After centrifuging for 3 min at 140,000 rpm, the supernatant was removed. The transfected EV pellet was suspended in 300 µl PBS and 150 µl of transfected EVs were added to 50'000 HUVECs cultivated in 6 wells. The same amounts of cel-miR-39 and Exo-Fect reagent were used as negative control.

To assess the pro-inflammatory effect of EVs, CD31+EVs were isolated from 1 ml of plasma from Ctrl, T2DM-NC, or T2DM-C, detached from beads, and used to treat 50'000 HUVECs cultivated in 6 wells for 24 hours. Messenger RNA measurement by RT-PCR was performed as previously described (38). Primers used were as previously reported (39).

Statistical analysis

Continuous variables were tested for normality using the Shapiro Wilk's test and reported as mean ± SD. To compare the expression of $CD31^+$ EV-shuttled miRNAs in the three different groups, Kruskal-Wallis followed by Dunn post hoc test was used, while to compare data from controls and T2DM patients Mann–Whitney U test was applied. Categorical variables were compared using the Chi-Squared test. Pearson's correlation was used to assess correlations between continuous variables. One-way ANCOVA was used to evaluate differences in continuous variables between groups while controlling for selected clinical and biochemical variables.

Multinomial logistic regression models were constructed to identify factors associated with the diagnosis of T2DM and its complications. A parsimonious backward-stepwise elimination of non-significant variables was deemed as appropriate in our setting. Model fit was assessed using the Hosmer-Lemeshow goodness-of-fit test. The proportion of variance explained by the final model was determined using the Nagelkerke R^2 statistic.

ROC curves were constructed for the single miRNAs and for the predicted probabilities derived from the logistic regression models. The Youden's index was used to calculate the best cut-off values, where appropriate. Multiple ROC curves were compared using the DeLong method (41).

The analyses were carried out using IBM SPSS Statistics, version 26 (IBM Corp, Armonk, NY, USA) and R, version 3.6.1. Statistical significance was defined as a two-tailed p-value <0.05.

Data and Resource Availability

Profiling raw data were deposited in GEO and are available with the accession number GSE142553. Data relative to EV isolation and characterization have been submitted to the EV-TRACK

knowledgebase (EV-TRACK ID: EV200038). All the other data generated during and/or analyzed during the current study are available from the corresponding author upon reasonable request.

RESULTS

Isolation and characterization of CD31$^+$ extracellular vesicles

After immunomagnetic capture from 1 ml of pooled plasma samples from control subjects (**Figure 1A**, details in methods), standard nanoparticles tracking analysis (NTA) was used to quantify our EV isolate. NTA revealed that our method is able to mostly isolate vesicles compatible with the size of small EVs (14) (**Figure 1B**). Isolated EVs were also characterized by TEM, which showed round-shaped vesicles with a minimal presence of contaminants (**Figure 1C**). To further characterize the collected EV population and to control their positivity for CD31, we compared this method with a standard approach to isolate EVs, *i.e.* ultracentrifugation (UC, at 120'000 *g*). We subjected EVs isolated from 1 ml of plasma to comparative analysis (from the same pooled control samples, n=6) for both Western Blot and surface markers expression with a specific kit to detect EV proteins through cytofluorimeter (35). As suggested by MISEV guidelines (14), EVs collected with CD31 beads were positive for EV-associated transmembrane, *i.e.* CD63 and CD31, and cytosolic, *i.e.* Alix and TSG101, proteins (**Figure 1D**). In addition, the CD31-beads method enriched the population of CD31+EVs compared to UC, as demonstrated by a higher ratio of CD31 over conventional EV markers. In addition, since lipoproteins are often isolated as contaminants with various EV isolation methods, we tested the expression of ApoA1 and ApoB100, two major components of lipoproteins. Albeit positive with both CD31 beads and UC, the immunomagnetic method was accompanied by a lower presence of these contaminants (**Figure 1D**). To substantiate these findings, the same comparison was subjected to cytofluorimetric detection of the EV markers CD9, CD63, and CD81, as well as of CD31. As expected, the CD31-beads method enriched the population of CD31$^+$EVs compared to UC, as demonstrated by an increased ratio of CD31 over EV surface markers in CD31$^+$ EVs compared to EVs isolated with UC (**Figure 1E**). To explore whether the use of beads for isolation is associated with a non-specific binding of EVs and to gain preliminary insights into the putative cell source of

CD31$^+$ EVs, we compared EVs isolated through CD31 beads to those eventually collected using beads with isotype control or using no beads, starting from the same amount of volume (1 ml, n=3) and using the same procedure. Cytofluorimetric detection of a large range of surface markers revealed a significantly higher expression of EV markers, but also of a large range of epitopes typical of platelets, *i.e.* CD41b and CD42a, and activated endothelial cells, *i.e.* CD62P. However, also CD49e, CD29, and CD69 (beyond tetraspanins) were significantly increased with CD31 beads. (**Figure 1F**). Indeed, all the other tested markers (35) were not expressed in our EVs (data not shown). To explore which fraction of total plasma EVs is represented by the isolated EVs, we collected the depleted fraction of the CD31 beads method and, after UC, subjected it to NTA comparison (control samples; n=3), which revealed that the concentration of collected CD31$^+$ EVs is significantly lower than its depleted counterpart (**Figure 1G**). In addition, we compared the surface markers expression of CD31$^+$EVs vs the CD31 depleted fraction. Results evidenced a higher abundance of the platelets marker CD41b and a lower positivity for common EVs markers, *i.e.* CD9, CD63, and CD81 in CD31$^+$EVs compared with the depleted fraction (**Supplementary Figure 1A**). To explore the yield efficiency of our isolation technique, we compared the abundance of CD31 in UC-isolated EVs, in isolated CD31$^+$EVs, and in the CD31 depleted fraction starting from the same samples processed in succession. We found no significant differences in the abundance of CD31 between the initial sample and CD31+EVs, while a significant decrease was observed in the CD31 depleted fraction compared with the initial sample (**Supplementary Figure 1B**). To test whether isolating CD31+ EVs yields quantitatively different results in terms of miRNA abundance compared to UC and to whole plasma (42; 43), the same amount of plasma was used for the isolation of CD31+EVs, EVs with UC, or left untreated (except for pre-clearance) and then these three samples were subjected to RNA extraction to quantify four miRNAs commonly studied in settings of T2DM and CVD, i.e. miR-126-3p, miR-146a-5p, miR-155, and miR-21-5p (10). All miRNAs were consistently expressed with the three tested approaches, being higher in total plasma, followed by EVs isolated through UC, and finally in CD31+EVs (**Figure 1H**), in line with the observation that CD31+EVs represent only a fraction of

total plasma EVs. Overall, these data suggest that our isolation method harvests CD31+ EVs, representing a fraction of plasma EVs with a heterogenous origin but compatible with the hypothesis that platelets and endothelial cells contribute to this specific EVs pool.

Comparative concentration, size and miRNA profiling of CD31$^+$ EVs from controls and patients with T2DM

To explore if T2DM affects the number and size of CD31$^+$ EVs, we compared four pooled samples from healthy controls with four pooled samples from patients with T2DM without complications (1ml each). NTA showed that the concentration of CD31+ EVs was not significantly affected by T2DM (**Figure 2A**), while a slight but significant decrease in their modal size was also observed (**Figure 2B**). Cytofluorimetric comparison of surface markers supported NTA data, since the expression of CD31, CD9, CD63, and CD81 was also slightly but not significantly increased in T2DM samples (n=4) (**Figure 2C**).

Then, we performed a comparative profiling of miRNA content within CD31$^+$EVs comparing Ctrl and T2DM patients (5 *vs* 5 samples with each sample prepared from pooled plasma). Of the 367 profiled miRNAs, 103 were detectable in at least one sample (**Figure 2D**), and 39 were expressed in 4 out of 5 (80%) of the tested samples. Comparison of Ctrl and T2DM evidenced a different relative quantity of miRNAs in CD31$^+$EVs (**Figure 2D**).

Diagnostic performance of a selected miRNA signature for T2DM status and complications

To explore the possible association of CD31$^+$EV-shuttled miRNAs with T2DM status and T2DM complications, we selected 11 miRNAs for two characteristics: 1. being proposed to play a role in the development of CV complications of T2DM or previously suggested to have diagnostic potential in CV studies (**Supplementary Table 1** for supporting literature) and 2. being robustly expressed in our setting of isolated CD31$^+$ EVs (**Figure 2B**). This selected panel was composed of miR-126-3p, miR-146a-5p, miR-155, miR-195-5p, miR-21-5p, miR-24-3p, miR-320a, miR-342-3p, miR-376a, miR-

422, and miR-451a. We quantified single miRNAs by qPCR in $CD31^+$ EVs isolated from plasma of a cross-sectional cohort of 218 individuals, including 60 healthy (Ctrl), 57 with uncomplicated T2DM (T2DM-NC), and 101 with T2DM and complications (T2DM-C). The clinical, anthropometrical, and biochemical variables of the subjects are reported in **Table 1**.

Analysis of the expression profiles among groups revealed significant differences for all the evaluated miRNAs, except miR-376a. **Supplementary Table 2** reports the relative expressions of the 11 miRNAs in each group, along with the results of the Student's *t* (CTR vs. T2DM) and one-way ANOVA (CTR vs. T2DM-NC vs. T2DM-C) tests, while **Figure 3** shows boxplots of the miRNA expression values across groups. Specifically, the circulating levels of 5 miRNAs, *i.e.* miR-21-5p, -146a, -342-3p, -422a, and -451a, are increased in T2DM patients, while 5 miRNAs, *i.e.* miR-24-3p, -126-3p, -155, -195-5p, and -320a, show decreased levels in T2DM. The post-hoc comparisons between the T2DM-NC and T2DM-C groups revealed significant differences for miR-21-5p, -146a, -342-3p, -422a and -451a (increased in T2DM-C); and for miR-320a (decreased in T2DM-C).

Therefore, ROC curves were generated to evaluate the diagnostic potential of these 10 miRNAs in detecting T2DM. Analysis of the ROC curves, showed in **Figure 4A**, revealed an outstanding diagnostic accuracy (AUC $\geq$ 0.90) for 5 miRNAs (list), and an excellent accuracy (0.80 $\leq$ AUC < 0.90) for 3 miRNAs (list). A second set of ROC curves was generated to assess the ability of the 6 miRNAs differentially regulated in T2DM-C vs. T2DM-NC to discriminate between the two groups. The diagnostic accuracy was acceptable for all of the 6 miRNAs, with AUCs ranging from 0.67 (miR-146a) to 0.80 (miR-342-3p) **(Figure 4B)**.

To test whether harvesting CD31+ EVs increases the ability of selected plasma miRNAs to detect T2DM and its complications, we compared the diagnostic performance of miR-146a-5p and miR-21-5p shuttled in CD31+ EVs with those of the same miRNAs quantified in the same amount of whole plasma. ROC curves indicate that CD31+EV-shuttled miR-146a-5p and miR-21-5p have a higher performance to detect both T2DM (AUC 0.911 vs 0.562, p<0.0001; and 0.859 vs 0.595, p<0.0001; respectively) (**Figure 4C**) and T2DM complications (AUC 0.673 vs 0.533, p=0.028; and 0.744 vs

0.511, p<0.001; respectively) compared to their whole plasma counterparts (**Figure 4D**), suggesting that the isolation of CD31+ EVs improve the diagnostic potential of plasma miR-146a-5p and miR-21-5p.

Diagnostic performance of the minimum miRNA signature for T2DM complications and major adverse cardiovascular events

To obtain the smallest possible signature with the highest discriminatory power for T2DM complications, we built a binary logistic regression to ascertain the effects of the 11 miRNAs, expressed as Z-scores, on the likelihood of complications in T2DM patients, with a backward stepwise procedure to achieve the most parsimonious model. The logistic regression model was statistically significant ($\chi^2(4) = 58.611$, $p < 0.001$) and explained 42.5% (Nagelkerke R^2) of the variance. Four miRNAs were retained into the model as significant predictors, *i.e.* miR-146a, -320a, -422a, -451a (**Supplementary Table 3**). A similar model was built including BMI and LDL-C as covariates, since these variables were not balanced between groups. As shown in **Supplementary Table 4**, inclusion of these covariates marginally affected the results.

Next, we tested the association between the 4-miRNA signature and the risk of MACE in T2DM patients. After inclusion in the model of HbA1c and the common risk factors age, gender, LDL-C, and hypertension as covariates, we still observed a strong association (p<0.001) between our signature and history of MACE. This logistic regression model was statistically significant ($\chi^2(6) = 102.960$, p<0.001) and explained 66.7% of the variance **(Table 2)**. To test whether this signature remains significant using a different normalization method (11), an additional logistic regression model was built after recalculating the signature using the global-mean (derived from all the quantified miRNAs)-normalized expression of 4 miRNAs. The regression model proved statistically significant ($\chi^2(6) = 86.572$, p<0.001, R^2=0.587) and included the 4-miRNA signature (p<0.001), increasing HbA1c (p=0.031) and male gender (p=0.044) as significant predictors of MACE **(Table 2)**.

To assess whether other CD31$^+$EV-shuttled miRNA signatures are associated to the development of MACE in T2DM patients, we built an additional logistic regression model with backward selection on the 11 miRNAs, including age, gender, LDL-C, HbA1c, and hypertension as covariates. Again, the logistic regression model was statistically significant ($\chi^2(7) = 155.777$, $p < 0.001$) and explained 87.3% of the variance. Of the 7 miRNAs which were retained into the model as predictors, 5 were statistically significant, *i.e.* miR-155, -320a, -342-3p, -376, and -422a. **Table 2** summarizes the model and shows the adjusted odds ratios (OR) for each miRNA.

To assess whether CD31$^+$EV-shuttled miRNAs associate with other complications of T2DM, multiple one-way ANCOVAs were computed to explore the relationship between the 11 miRNAs and T2DM complications after adjusting for age and gender. **Supplementary Table 5** reports the adjusted means for each miRNA in subjects with or without a specific complication. We observed a significant differential regulation of all the CD31$^+$EV-shuttled miRNAs, except miR-126, in macrovascular complications, *i.e.* peripheral artery disease and MACE. The association between the levels of 9 miRNAs and MACE remained significant even after adjustment for HbA1c and the presence of other concomitant T2DM complications. On the contrary, no significant association was found between miRNAs and any of the microvascular complications**.**Since blood miRNAs and especially platelet derived miRNAs have been shown to be affected by anti-platelet therapies (47), we explored whether anti-platelet medications affected our results. However, we did not observe any significant effect of anti-platelet therapy on miRNA expression (data not shown).

Correlations with clinical variables and between miRNAs

We then explored the association between the 11 CD31$^+$EV-shuttled miRNAs and a large range of relevant biochemical and clinical variables. The resulting color-coded correlation plot is shown in **Figure 5A**. The correlation coefficient ranged from -0.51 to 0.40. A similar correlation plot was drawn to highlight reciprocal correlations between the levels of the 11 miRNAs under investigation (**Figure 5B**). The complete correlation matrix is reported in **Supplementary Table 6**. Notably, the levels of all the T2DM-associated miRNAs, except miR-320a, are linearly related with fasting

glucose and, among these, 7 miRNAs correlate also with HbA1c, whereas only 2 miRNAs correlate with homeostatic model assessment-insulin resistance (HOMA-IR). While our miRNA signature showed no significant association with the presence of diabetic nephropathy, 9 miRNAs are linearly related to either serum creatinine, azotemia, or eGFR, with the direction of the correlation being concordant with the expected deterioration of the renal function with worsening glycemic control. Eight miRNAs showed an association with age, with 6 miRNAs also being inversely correlated with PBMC telomere length. In addition, we observed a remarkable pattern of correlations between 8 miRNAs and the lipid profile. Of note, 7 out of 8 of these miRNAs showed also a correlation with waist/hip ratio, fasting glucose, and HbA1c with an inverse trend when compared to their correlation with lipid profile, suggesting a divergent effect of common CV risk factors on these variables. Overall, these data indicate that $CD31^+$EV-shuttled miRNAs may sense a wide range of common risk factors known to be key drivers of T2DM complications development. Finally, many of the miRNAs were significantly associated with one another (**Figure 5B**), extending the knowledge that circulating miRNAs are highly correlated also to those shuttled by $CD31^+$EVs (11).

$CD31^+$ EVs from patients with T2DM promote inflammation in endothelial cells *in vitro*

To explore whether the altered miRNA cargo of $CD31^+$ EVs derived from patients with T2DM affects the functional properties of these EVs when administered *in vitro* to endothelial cells, we unbounded collected EVs from beads with a commercially available buffer and the help of a magnet (**Figure 6A**, details in methods). First, we verified the ability of endothelial cells to uptake EVs stained with a fluorescent dye after a 24h incubation (**Figure 6B,** representative image of a n = 3 EVs preparation from control samples). Since fluorescent dyes might be accompanied by non-specific binding to the lipidic components of the cells (64), we loaded a small RNA with a red fluorophore into EVs and then used them to treat endothelial cells. We detected a consistent red fluorescence in recipient cells, suggesting that collected EVs were able to deliver small RNAs to recipient endothelial cells (**Figure 6C**). To support this observation, we administer EVs transfected with a non-human miRNA, *i.e.* cel-miR-39, to endothelial cells (n=3, EVs isolated from control samples). The same amount of EV-free,

cel-miR-39 (along with the transfecting reagent), PBS, and non-transfected EVs were used as negative controls. As shown in **Figure 6D**, cel-miR-39 expression was higher in endothelial cells treated with transfected EVs compared to the same amount of this miRNA not loaded onto EVs, while cel-miR-39 was undetectable in the other two negative controls (data not shown). Given that many of the $CD31^+$ EV miRNAs found to be altered by T2DM and its complications (**Figure 3**) have been previously associated with the alteration of inflammatory pathways (16; 25), we treated endothelial cells with $CD31^+$ EVs derived from control, T2DM-NC, and T2DM-C (n=3 each, from 1 ml of plasma) and measured the expression of a panel of pro-inflammatory genes at the mRNA level. EVs from both T2DM-NC and T2DM-C significantly increased the expression of chemokine (C-C motif) ligand 2 (*CCL2*, also referred to as monocyte chemoattractant protein-1, *i.e. MCP-1*) and interleukin 1α *(IL-1α)* when compared to EVs from control subjects, while only EVs from T2DM-C induced the expression of *TNFα* in recipient endothelial cells when compared to both T2DM-NC and controls. Finally, the expression of *IL-6*, chemokine (C-X-C motif) ligand (*CXCL*)*-1*, and *CXCL-8* was not affected by any of the treatments (**Figure 6E**), possibly suggesting a peculiar pro-inflammatory effect of EVs, rather than a non-specific inflammatory response.

DISCUSSION

Circulating miRNA quantification has already been proposed as a potential approach to evaluate CV risk (47-49). However, while data on circulating miRNAs in the setting of CV diagnostic for the general population are promising (47), none of the miRNAs has been translated into the clinic for diagnostic purposes, including in the context of T2DM-related complications. Lack of standardization methods and the complex contribution of different tissues and pathological processes to circulating miRNA pool are among the reasons that limit their use (10; 11). To overcome these issues, the quantification in specific miRNA cargos has been proposed. Indeed, microvesicle (MV)-shuttled miR-126 and miR-199a but not freely circulating miRNA expression predict the occurrence of CV events in patients with stable coronary artery disease (18), while T2DM patients with prevalent CVD show low miR-26a and miR-126 levels within large MVs (50). In particular, it was suggested that

MV-shuttled miRNAs derive from endothelial cells (18; 51), while the most abundant miRNAs in whole plasma are among those highly expressed in platelets (7; 44; 52). However, since a seminal paper indicated that the majority of exosomal (*i.e.* small EVs) miRNAs derive from adipose tissue (24), we decided to harvest EVs expressing CD31, in order to enrich EVs derived from platelets, endothelial cells, and immune cells, *i.e.* the most relevant cellular components in the etiopathogenesis of T2DM complications. We showed here that the isolation of $CD31^+$ EVs results in a EVs pool compatible with a platelet and endothelial cell origin, as shown by analysis of surface markers expression. However, since also other markers were positive, the origin of collected EVs is likely heterogenous.

A recent study has characterized the abundance and functional alterations of circulating EVs from patients with T2DM, showing a higher plasma EV concentration in individuals with diabetes, an observation obtained by isolating EVs with both a commercial kit and UC (53). However, when comparing surface marker expression, erythrocyte-derived EVs were significantly increased by T2DM, while a non-significant trend was observed for platelets/endothelial cells derived particles (53), an observation compatible with our results. In addition, the same study showed that EVs from patients with T2DM are able to induce an inflammatory response in recipient monocytes *in vitro*. Another study found that also EVs from patients with gestational diabetes promote inflammation when administered to endothelial cells (55). Here, we extend these findings by showing that also $CD31^+$ EVs from patients with T2DM are able to foster low-grade inflammation in recipient endothelial cells, with a variable effect when considering T2DM with or without complications. Given that EVs can shuttle a large repertoire of molecules, research aimed at studying the specific components fostering inflammatory pathways might provide useful information for the etiopathogenesis of the disease, especially considering that low-grade inflammation is associated with the presence of T2DM complications (56). To our knowledge, only one study used the CD31 beads approach to isolate EVs from patients with T2DM (57). In that study, $CD31^+$ EVs were shown to

boost apoptosis resistance of vascular smooth muscle cells cultured in hyperglycaemic condition, an effect possibly mediated by membrane-bound platelet-derived growth factor-BB.

Few studies quantified miRNA abundance within EVs in diabetic cohorts (21; 22; 58; 48,50). Interestingly, two studies found an increased abundance of miR-126-3p in EVs from T2DM patients (22; 23), while here a slightly decreasing trend was observed for $CD31^{+}$EV-shuttled miR-126-3p. This miRNA was previously suggested as one of the most downregulated miRNAs when analysing whole plasma or large endothelial MVs (9; 18; 59). On the contrary, miR-21-5p in $CD31^{+}$EVs showed an opposite trend compared to the previously observed decrease in plasma of T2DM patients, but not in total EVs (9; 59). Assuming that $CD31^{+}$ EVs derive mainly from platelets and endothelial cells, our results might appear consistent with the observation that hyperglycaemia induced a downregulation of mir-126-3p in endothelial EVs (18) and in platelets (60). The two studies finding an increased expression of miR-126-3p (22; 23) were performed using different isolation methods that collect a broader EV population, possibly suggesting that the effect of T2DM on miR-126-3p expression is divergent when considering different tissues. Indeed, two different mouse models of insulin resistance showed an increased expression of miR-126-3p in the liver (61) and in the adipose tissue (62). Considering also that the majority of plasma EV miRNAs are held to derive form adipose tissue (24), it is conceivable that a broad, non-tissue specific EVs collection method provides opposite results if compared with an immunomagnetic method likely enriching for tissue-specific EVs. On the other side, miR-21-5p shuttled in total EVs is increased in T2DM patients with diabetic nephropathy compared to non-complicated patients (23), similarly to our observation when considering CD31+ EVs-shuttled miR-21-5p and T2DM complications as a whole. Notably, even though miR-21-5p shuttled in $CD31^{+}$ EVs was not associated with prevalent nephropathy in our cohort, its levels were correlated with multiple measures of kidney function. All these observations suggest that harvesting rare EV fractions or subpopulations might hold an increased potential for miRNA-biomarker discovery if compared to broader EV collections or to whole plasma, possibly limiting the heterogeneous, pleiotropic effect of T2DM on the expression of miRNAs at the tissue

level. The results showing an increased performance of CD31$^+$EV-shuttled miR-21-5p and miR-146a-5p compared to the whole plasma levels of the same miRNAs in detecting both T2DM and its complications might support this hypothesis.

Limitations of the study

The main limitation of this study is that we used a cross-sectional cohort, thus we cannot determine if the obtained signature is able to longitudinally identify patients at risk of T2DM complications or specifically MACE. Moreover, given this study design, we cannot perform a direct comparison with already available tools. In addition, the BMI of patients with T2DM was significantly higher compared to controls. However, since we isolated a specific fraction of EVs, the concentration of which was not affected by T2DM, it is unlikely that the observed differences in miRNA abundance are solely ascribable to the diverse quantity of adipose tissue between T2DM patients and controls. In addition, plasma isolation was performed with a low centrifugation speed, which might have left residual platelets in the samples that could have been then activated by thawing. However, before magnetic isolation, samples were precleared with two subsequent centrifugations, thus minimizing the risk of a consistent contamination by platelets granules or fragments. Finally, we did not perform functional experiments to explore which components of the EV-cargo are responsible of the observed pro-inflammatory effect.

Conclusions

In summary, we have here isolated CD31$^+$EVs in a large cohort of T2DM patients showing that specific miRNA signatures associate with T2DM complications as a whole or individually with MACE. We also show that harvesting CD31$^+$ EVs, compared to whole plasma, improves the ability of miR-21-5p and miR-146a-5p to detect T2DM and its complications. Finally, we also demonstrated that CD31$^+$ EVs from T2DM patients are endowed with pro-inflammatory properties when administered *in vitro* to endothelial cells, overall encouraging further research to explore both the diagnostic potential and the functional role of T2DM-driven EV alterations.

ACKNOWLEDGMENTS

Author Contributions

F.P., F.O., and A.C. conceived the idea and designed the study. V.d.N. performed the majority of experiments. J.S. and A.G. performed statistical analysis and prepared figures and tables. R.S. and E. M. performed miRNA profiling and Western Blot experiments. C.C., M.P, and I.C. performed cytofluorimeter and TEM experiments. A.G., N.B., M.R.R., A.R.B., L.L.S., A.D.P., S.G., G.M., A.N, and P.d.C revised the paper for intellectual content and provided additional expertise. F.P., J.S, F.O., and A.C wrote the paper. The final version of the manuscript was approved by all authors.

F.P. is the guarantor of this work and, as such, had full access to all the data in the study and takes responsibility for the integrity of the data and the accuracy of the data analysis.

Conflict of interest

None of the authors have competing interests.

Sources of funding

This work was supported by grants from La Maratò de TV3 to A.C and by the Italian Ministry of Health (Ricerca Corrente) to IRCCS MultiMedica.

REFERENCES

1. DeFronzo RA, Ferrannini E, Groop L, Henry RR, Herman WH, Holst JJ, Hu FB, Kahn CR, Raz I, Shulman GI, Simonson DC, Testa MA, Weiss R: Type 2 diabetes mellitus. Nat Rev Dis Primers 2015;1:15019

2. Dal Canto E, Ceriello A, Ryden L, Ferrini M, Hansen TB, Schnell O, Standl E, Beulens JW: Diabetes as a cardiovascular risk factor: An overview of global trends of macro and micro vascular complications. Eur J Prev Cardiol 2019;26:25-32

3. Gaede P, Lund-Andersen H, Parving HH, Pedersen O: Effect of a multifactorial intervention on mortality in type 2 diabetes. N Engl J Med 2008;358:580-591

4. Bachmann KN, Wang TJ: Biomarkers of cardiovascular disease: contributions to risk prediction in individuals with diabetes. Diabetologia 2018;61:987-995

5. Willeit P, Skroblin P, Moschen AR, Yin X, Kaudewitz D, Zampetaki A, Barwari T, Whitehead M, Ramirez CM, Goedeke L, Rotllan N, Bonora E, Hughes AD, Santer P, Fernandez-Hernando C, Tilg H, Willeit J, Kiechl S, Mayr M: Circulating MicroRNA-122 Is Associated With the Risk of New-Onset Metabolic Syndrome and Type 2 Diabetes. Diabetes 2017;66:347-357

6. Zampetaki A, Mayr M: Sweet dicer: impairment of micro-RNA processing by diabetes. Circ Res 2015;117:116-118

7. Mayr M, Zampetaki A, Kiechl S: MicroRNA biomarkers for failing hearts? Eur Heart J 2013;34:2782-2783

8. Zampetaki A, Willeit P, Drozdov I, Kiechl S, Mayr M: Profiling of circulating microRNAs: from single biomarkers to re-wired networks. Cardiovasc Res 2012;93:555-562

9. Olivieri F, Spazzafumo L, Bonafe M, Recchioni R, Prattichizzo F, Marcheselli F, Micolucci L, Mensa E, Giuliani A, Santini G, Gobbi M, Lazzarini R, Boemi M, Testa R, Antonicelli R, Procopio AD, Bonfigli AR: MiR-21-5p and miR-126a-3p levels in plasma and circulating angiogenic cells: relationship with type 2 diabetes complications. Oncotarget 2015;6:35372-35382

10. Prattichizzo F, Giuliani A, De Nigris V, Pujadas G, Ceka A, La Sala L, Genovese S, Testa R, Procopio AD, Olivieri F, Ceriello A: Extracellular microRNAs and endothelial hyperglycaemic memory: a therapeutic opportunity? Diabetes Obes Metab 2016;18:855-867

11. Sunderland N, Skroblin P, Barwari T, Huntley RP, Lu R, Joshi A, Lovering RC, Mayr M: MicroRNA Biomarkers and Platelet Reactivity: The Clot Thickens. Circ Res 2017;120:418-435

12. Coumans FAW, Brisson AR, Buzas EI, Dignat-George F, Drees EEE, El-Andaloussi S, Emanueli C, Gasecka A, Hendrix A, Hill AF, Lacroix R, Lee Y, van Leeuwen TG, Mackman N, Mager I, Nolan JP, van der Pol E, Pegtel DM, Sahoo S, Siljander PRM, Sturk G, de Wever O, Nieuwland R: Methodological Guidelines to Study Extracellular Vesicles. Circ Res 2017;120:1632-1648

13. Witwer KW, Thery C: Extracellular vesicles or exosomes? On primacy, precision, and popularity influencing a choice of nomenclature. J Extracell Vesicles 2019;8:1648167

14. Thery C, Witwer KW, Aikawa E, Alcaraz MJ, Anderson JD, Andriantsitohaina R, Antoniou A, Arab T, Archer F, Atkin-Smith GK, Ayre DC, Bach JM, Bachurski D, Baharvand H, Balaj L, Baldacchino S, Bauer NN, Baxter AA, Bebawy M, Beckham C, Bedina Zavec A, Benmoussa A, Berardi AC, Bergese P, Bielska E, Blenkiron C, Bobis-Wozowicz S, Boilard E, Boireau W, Bongiovanni A, Borras FE, Bosch S, Boulanger CM, Breakefield X, Breglio AM, Brennan MA, Brigstock DR, Brisson A, Broekman ML, Bromberg JF, Bryl-Gorecka P, Buch S, Buck AH, Burger D, Busatto S, Buschmann D, Bussolati B, Buzas EI, Byrd JB, Camussi G, Carter DR, Caruso S, Chamley LW, Chang YT, Chen C, Chen S, Cheng L, Chin AR, Clayton A, Clerici SP, Cocks A, Cocucci E, Coffey RJ, Cordeiro-da-Silva A, Couch Y, Coumans FA, Coyle B, Crescitelli R, Criado MF, D'Souza-Schorey C, Das S, Datta Chaudhuri A, de Candia P, De Santana EF, De Wever O, Del Portillo HA, Demaret T, Deville S, Devitt A, Dhondt B, Di Vizio D, Dieterich LC, Dolo V, Dominguez Rubio

AP, Dominici M, Dourado MR, Driedonks TA, Duarte FV, Duncan HM, Eichenberger RM, Ekstrom K, El Andaloussi S, Elie-Caille C, Erdbrugger U, Falcon-Perez JM, Fatima F, Fish JE, Flores-Bellver M, Forsonits A, Frelet-Barrand A, Fricke F, Fuhrmann G, Gabrielsson S, Gamez-Valero A, Gardiner C, Gartner K, Gaudin R, Gho YS, Giebel B, Gilbert C, Gimona M, Giusti I, Goberdhan DC, Gorgens A, Gorski SM, Greening DW, Gross JC, Gualerzi A, Gupta GN, Gustafson D, Handberg A, Haraszti RA, Harrison P, Hegyesi H, Hendrix A, Hill AF, Hochberg FH, Hoffmann KF, Holder B, Holthofer H, Hosseinkhani B, Hu G, Huang Y, Huber V, Hunt S, Ibrahim AG, Ikezu T, Inal JM, Isin M, Ivanova A, Jackson HK, Jacobsen S, Jay SM, Jayachandran M, Jenster G, Jiang L, Johnson SM, Jones JC, Jong A, Jovanovic-Talisman T, Jung S, Kalluri R, Kano SI, Kaur S, Kawamura Y, Keller ET, Khamari D, Khomyakova E, Khvorova A, Kierulf P, Kim KP, Kislinger T, Klingeborn M, Klinke DJ, 2nd, Kornek M, Kosanovic MM, Kovacs AF, Kramer-Albers EM, Krasemann S, Krause M, Kurochkin IV, Kusuma GD, Kuypers S, Laitinen S, Langevin SM, Languino LR, Lannigan J, Lasser C, Laurent LC, Lavieu G, Lazaro-Ibanez E, Le Lay S, Lee MS, Lee YXF, Lemos DS, Lenassi M, Leszczynska A, Li IT, Liao K, Libregts SF, Ligeti E, Lim R, Lim SK, Line A, Linnemannstons K, Llorente A, Lombard CA, Lorenowicz MJ, Lorincz AM, Lotvall J, Lovett J, Lowry MC, Loyer X, Lu Q, Lukomska B, Lunavat TR, Maas SL, Malhi H, Marcilla A, Mariani J, Mariscal J, Martens-Uzunova ES, Martin-Jaular L, Martinez MC, Martins VR, Mathieu M, Mathivanan S, Maugeri M, McGinnis LK, McVey MJ, Meckes DG, Jr., Meehan KL, Mertens I, Minciacchi VR, Moller A, Moller Jorgensen M, Morales-Kastresana A, Morhayim J, Mullier F, Muraca M, Musante L, Mussack V, Muth DC, Myburgh KH, Najrana T, Nawaz M, Nazarenko I, Nejsum P, Neri C, Neri T, Nieuwland R, Nimrichter L, Nolan JP, Nolte-'t Hoen EN, Noren Hooten N, O'Driscoll L, O'Grady T, O'Loghlen A, Ochiya T, Olivier M, Ortiz A, Ortiz LA, Osteikoetxea X, Ostergaard O, Ostrowski M, Park J, Pegtel DM, Peinado H, Perut F, Pfaffl MW, Phinney DG, Pieters BC, Pink RC, Pisetsky DS, Pogge von Strandmann E, Polakovicova I, Poon IK, Powell BH, Prada I, Pulliam L, Quesenberry P, Radeghieri A, Raffai RL, Raimondo S, Rak J, Ramirez MI, Raposo G, Rayyan MS, Regev-Rudzki N, Ricklefs FL, Robbins PD, Roberts DD, Rodrigues SC, Rohde E, Rome S, Rouschop KM, Rughetti A, Russell AE, Saa P, Sahoo S, Salas-Huenuleo E, Sanchez C, Saugstad JA, Saul MJ, Schiffelers RM, Schneider R, Schoyen TH, Scott A, Shahaj E, Sharma S, Shatnyeva O, Shekari F, Shelke GV, Shetty AK, Shiba K, Siljander PR, Silva AM, Skowronek A, Snyder OL, 2nd, Soares RP, Sodar BW, Soekmadji C, Sotillo J, Stahl PD, Stoorvogel W, Stott SL, Strasser EF, Swift S, Tahara H, Tewari M, Timms K, Tiwari S, Tixeira R, Tkach M, Toh WS, Tomasini R, Torrecilhas AC, Tosar JP, Toxavidis V, Urbanelli L, Vader P, van Balkom BW, van der Grein SG, Van Deun J, van Herwijnen MJ, Van Keuren-Jensen K, van Niel G, van Royen ME, van Wijnen AJ, Vasconcelos MH, Vechetti IJ, Jr., Veit TD, Vella LJ, Velot E, Verweij FJ, Vestad B, Vinas JL, Visnovitz T, Vukman KV, Wahlgren J, Watson DC, Wauben MH, Weaver A, Webber JP, Weber V, Wehman AM, Weiss DJ, Welsh JA, Wendt S, Wheelock AM, Wiener Z, Witte L, Wolfram J, Xagorari A, Xander P, Xu J, Yan X, Yanez-Mo M, Yin H, Yuana Y, Zappulli V, Zarubova J, Zekas V, Zhang JY, Zhao Z, Zheng L, Zheutlin AR, Zickler AM, Zimmermann P, Zivkovic AM, Zocco D, Zuba-Surma EK: Minimal information for studies of extracellular vesicles 2018 (MISEV2018): a position statement of the International Society for Extracellular Vesicles and update of the MISEV2014 guidelines. J Extracell Vesicles 2018;7:1535750

15. Prattichizzo F, Giuliani A, Sabbatinelli J, Mensa E, De Nigris V, La Sala L, de Candia P, Olivieri F, Ceriello A: Extracellular vesicles circulating in young organisms promote healthy longevity. J Extracell Vesicles 2019;8:1656044

16. Prattichizzo F, Micolucci L, Cricca M, De Carolis S, Mensa E, Ceriello A, Procopio AD, Bonafe M, Olivieri F: Exosome-based immunomodulation during aging: A nano-perspective on inflamm-aging. Mech Ageing Dev 2017;168:44-53

17. Xiao Y, Zheng L, Zou X, Wang J, Zhong J, Zhong T: Extracellular vesicles in type 2 diabetes mellitus: key roles in pathogenesis, complications, and therapy. J Extracell Vesicles 2019;8:1625677

18. Jansen F, Yang X, Hoelscher M, Cattelan A, Schmitz T, Proebsting S, Wenzel D, Vosen S, Franklin BS, Fleischmann BK, Nickenig G, Werner N: Endothelial microparticle-mediated transfer of MicroRNA-126 promotes vascular endothelial cell repair via SPRED1 and is abrogated in glucose-damaged endothelial microparticles. Circulation 2013;128:2026-2038

19. Sun Y, Shi H, Yin S, Ji C, Zhang X, Zhang B, Wu P, Shi Y, Mao F, Yan Y, Xu W, Qian H: Human Mesenchymal Stem Cell Derived Exosomes Alleviate Type 2 Diabetes Mellitus by Reversing Peripheral Insulin Resistance and Relieving beta-Cell Destruction. ACS Nano 2018;12:7613-7628

20. Castano C, Novials A, Parrizas M: Exosomes and diabetes. Diabetes Metab Res Rev 2019;35:e3107

21. Katayama M, Wiklander OPB, Fritz T, Caidahl K, El-Andaloussi S, Zierath JR, Krook A: Circulating Exosomal miR-20b-5p Is Elevated in Type 2 Diabetes and Could Impair Insulin Action in Human Skeletal Muscle. Diabetes 2019;68:515-526

22. Ghai V, Kim TK, Etheridge A, Nielsen T, Hansen T, Pedersen O, Galas D, Wang K: Extracellular Vesicle Encapsulated MicroRNAs in Patients with Type 2 Diabetes Are Affected by Metformin Treatment. J Clin Med 2019;8

23. Florijn BW, Duijs J, Levels JH, Dallinga-Thie GM, Wang Y, Boing AN, Yuana Y, Stam W, Limpens R, Au YW, Nieuwland R, Rabelink TJ, Reinders MEJ, van Zonneveld AJ, Bijkerk R: Diabetic Nephropathy Alters the Distribution of Circulating Angiogenic MicroRNAs Among Extracellular Vesicles, HDL, and Ago-2. Diabetes 2019;68:2287-2300

24. Thomou T, Mori MA, Dreyfuss JM, Konishi M, Sakaguchi M, Wolfrum C, Rao TN, Winnay JN, Garcia-Martin R, Grinspoon SK, Gorden P, Kahn CR: Adipose-derived circulating miRNAs regulate gene expression in other tissues. Nature 2017;542:450-455

25. Prattichizzo F, De Nigris V, Spiga R, Mancuso E, La Sala L, Antonicelli R, Testa R, Procopio AD, Olivieri F, Ceriello A: Inflammageing and metaflammation: The yin and yang of type 2 diabetes. Ageing Res Rev 2018;41:1-17

26. Kaur R, Kaur M, Singh J: Endothelial dysfunction and platelet hyperactivity in type 2 diabetes mellitus: molecular insights and therapeutic strategies. Cardiovasc Diabetol 2018;17:121

27. Clayton A, Court J, Navabi H, Adams M, Mason MD, Hobot JA, Newman GR, Jasani B: Analysis of antigen presenting cell derived exosomes, based on immuno-magnetic isolation and flow cytometry. J Immunol Methods 2001;247:163-174

28. Testa R, Olivieri F, Sirolla C, Spazzafumo L, Rippo MR, Marra M, Bonfigli AR, Ceriello A, Antonicelli R, Franceschi C, Castellucci C, Testa I, Procopio AD: Leukocyte telomere length is associated with complications of type 2 diabetes mellitus. Diabet Med 2011;28:1388-1394

29. American Diabetes A: 2. Classification and Diagnosis of Diabetes: Standards of Medical Care in Diabetes-2019. Diabetes Care 2019;42:S13-S28

30. Testa R, Bonfigli AR, Salvioli S, Invidia L, Pierini M, Sirolla C, Marra M, Testa I, Fazioli F, Recchioni R, Marcheselli F, Olivieri F, Lanari L, Franceschi C: The Pro/Pro genotype of the p53 codon 72 polymorphism modulates PAI-1 plasma levels in ageing. Mech Ageing Dev 2009;130:497-500

31. Olivieri F, Bonafe M, Spazzafumo L, Gobbi M, Prattichizzo F, Recchioni R, Marcheselli F, La Sala L, Galeazzi R, Rippo MR, Fulgenzi G, Angelini S, Lazzarini R, Bonfigli AR, Bruge F, Tiano L, Genovese S, Ceriello A, Boemi M, Franceschi C, Procopio AD, Testa R: Age- and glycemia-related miR-126-3p levels in plasma and endothelial cells. Aging (Albany NY) 2014;6:771-787

32. Mensa E, Giuliani A, Matacchione G, Gurau F, Bonfigli AR, Romagnoli F, De Luca M, Sabbatinelli J, Olivieri F: Circulating miR-146a in healthy aging and type 2 diabetes: Age- and gender-specific trajectories. Mech Ageing Dev 2019;180:1-10

33. Consortium E-T, Van Deun J, Mestdagh P, Agostinis P, Akay O, Anand S, Anckaert J, Martinez ZA, Baetens T, Beghein E, Bertier L, Berx G, Boere J, Boukouris S, Bremer M, Buschmann D, Byrd JB, Casert C, Cheng L, Cmoch A, Daveloose D, De Smedt E, Demirsoy S, Depoorter V, Dhondt B, Driedonks TA, Dudek A, Elsharawy A, Floris I, Foers AD, Gartner K, Garg AD, Geeurickx E, Gettemans J, Ghazavi F, Giebel B, Kormelink TG, Hancock G, Helsmoortel H, Hill AF, Hyenne V, Kalra H, Kim D, Kowal J, Kraemer S, Leidinger P, Leonelli C, Liang Y, Lippens L, Liu S, Lo Cicero A, Martin S, Mathivanan S, Mathiyalagan P, Matusek T, Milani G, Monguio-Tortajada M, Mus LM, Muth DC, Nemeth A, Nolte-'t Hoen EN, O'Driscoll L, Palmulli R, Pfaffl MW, Primdal-Bengtson B, Romano E, Rousseau Q, Sahoo S, Sampaio N, Samuel M,

Scicluna B, Soen B, Steels A, Swinnen JV, Takatalo M, Thaminy S, Thery C, Tulkens J, Van Audenhove I, van der Grein S, Van Goethem A, van Herwijnen MJ, Van Niel G, Van Roy N, Van Vliet AR, Vandamme N, Vanhauwaert S, Vergauwen G, Verweij F, Wallaert A, Wauben M, Witwer KW, Zonneveld MI, De Wever O, Vandesompele J, Hendrix A: EV-TRACK: transparent reporting and centralizing knowledge in extracellular vesicle research. Nat Methods 2017;14:228-232

34. Gardiner C, Ferreira YJ, Dragovic RA, Redman CW, Sargent IL: Extracellular vesicle sizing and enumeration by nanoparticle tracking analysis. J Extracell Vesicles 2013;2

35. Koliha N, Wiencek Y, Heider U, Jungst C, Kladt N, Krauthauser S, Johnston IC, Bosio A, Schauss A, Wild S: A novel multiplex bead-based platform highlights the diversity of extracellular vesicles. J Extracell Vesicles 2016;5:29975

36. Metsalu T, Vilo J: ClustVis: a web tool for visualizing clustering of multivariate data using Principal Component Analysis and heatmap. Nucleic Acids Res 2015;43:W566-570

37. Heberle H, Meirelles GV, da Silva FR, Telles GP, Minghim R: InteractiVenn: a web-based tool for the analysis of sets through Venn diagrams. BMC Bioinformatics 2015;16:169

38. Mensà E, Guescini M, Giuliani A, Bacalini MG, Ramini D, Corleone G, Ferracin M, Fulgenzi G, Graciotti L, Prattichizzo F, Sorci L, Battistelli M, Monsurrò V, Bonfigli AR, Cardelli M, Recchioni R, Marcheselli F, Latini S, Maggio S, Fanelli M, Amatori S, Storci G, Ceriello A, Stocchi V, De Luca M, Magnani L, Rippo MR, Procopio AD, Sala C, Budimir I, Bassi C, Negrini M, Garagnani P, Franceschi C, Sabbatinelli J, Bonafè M, Olivieri F: Small extracellular vesicles deliver miR-21 and miR-217 as pro-senescence effectors to endothelial cells. Journal of Extracellular Vesicles 2020;9:1725285

39. Prattichizzo F, De Nigris V, Mancuso E, Spiga R, Giuliani A, Matacchione G, Lazzarini R, Marcheselli F, Recchioni R, Testa R, La Sala L, Rippo MR, Procopio AD, Olivieri F, Ceriello A: Short-term sustained hyperglycaemia fosters an archetypal senescence-associated secretory phenotype in endothelial cells and macrophages. Redox Biol 2018;15:170-181

40. Keller A, Fehlmann T, Ludwig N, Kahraman M, Laufer T, Backes C, Vogelmeier C, Diener C, Biertz F, Herr C, Jorres RA, Lenhof HP, Meese E, Bals R, Group CS: Genome-wide MicroRNA Expression Profiles in COPD: Early Predictors for Cancer Development. Genomics Proteomics Bioinformatics 2018;16:162-171

41. DeLong ER, DeLong DM, Clarke-Pearson DL: Comparing the areas under two or more correlated receiver operating characteristic curves: a nonparametric approach. Biometrics 1988;44:837-845

42. Turchinovich A, Samatov TR, Tonevitsky AG, Burwinkel B: Circulating miRNAs: cell-cell communication function? Front Genet 2013;4:119

43. Turchinovich A, Weiz L, Langheinz A, Burwinkel B: Characterization of extracellular circulating microRNA. Nucleic Acids Res 2011;39:7223-7233

44. Kaudewitz D, Skroblin P, Bender LH, Barwari T, Willeit P, Pechlaner R, Sunderland NP, Willeit K, Morton AC, Armstrong PC, Chan MV, Lu R, Yin X, Gracio F, Dudek K, Langley SR, Zampetaki A, de Rinaldis E, Ye S, Warner TD, Saxena A, Kiechl S, Storey RF, Mayr M: Association of MicroRNAs and YRNAs With Platelet Function. Circ Res 2016;118:420-432

45. van Balkom BW, Eisele AS, Pegtel DM, Bervoets S, Verhaar MC: Quantitative and qualitative analysis of small RNAs in human endothelial cells and exosomes provides insights into localized RNA processing, degradation and sorting. J Extracell Vesicles 2015;4:26760

46. Sharma H, Chinnappan M, Agarwal S, Dalvi P, Gunewardena S, O'Brien-Ladner A, Dhillon NK: Macrophage-derived extracellular vesicles mediate smooth muscle hyperplasia: role of altered miRNA cargo in response to HIV infection and substance abuse. FASEB J 2018;32:5174-5185

47. Willeit P, Zampetaki A, Dudek K, Kaudewitz D, King A, Kirkby NS, Crosby-Nwaobi R, Prokopi M, Drozdov I, Langley SR, Sivaprasad S, Markus HS, Mitchell JA, Warner TD, Kiechl S, Mayr M: Circulating microRNAs as novel biomarkers for platelet activation. Circ Res 2013;112:595-600

48. Barwari T, Joshi A, Mayr M: MicroRNAs in Cardiovascular Disease. J Am Coll Cardiol 2016;68:2577-2584

49. Willeit P, Skroblin P, Kiechl S, Fernandez-Hernando C, Mayr M: Liver microRNAs: potential mediators and biomarkers for metabolic and cardiovascular disease? Eur Heart J 2016;37:3260-3266

50. Jansen F, Wang H, Przybilla D, Franklin BS, Dolf A, Pfeifer P, Schmitz T, Flender A, Endl E, Nickenig G, Werner N: Vascular endothelial microparticles-incorporated microRNAs are altered in patients with diabetes mellitus. Cardiovasc Diabetol 2016;15:49

51. Jansen F, Li Q, Pfeifer A, Werner N: Endothelial- and Immune Cell-Derived Extracellular Vesicles in the Regulation of Cardiovascular Health and Disease. JACC Basic Transl Sci 2017;2:790-807

52. Zampetaki A, Willeit P, Tilling L, Drozdov I, Prokopi M, Renard JM, Mayr A, Weger S, Schett G, Shah A, Boulanger CM, Willeit J, Chowienczyk PJ, Kiechl S, Mayr M: Prospective study on circulating MicroRNAs and risk of myocardial infarction. J Am Coll Cardiol 2012;60:290-299

53. Freeman DW, Noren Hooten N, Eitan E, Green J, Mode NA, Bodogai M, Zhang Y, Lehrmann E, Zonderman AB, Biragyn A, Egan J, Becker KG, Mattson MP, Ejiogu N, Evans MK: Altered Extracellular Vesicle Concentration, Cargo, and Function in Diabetes. Diabetes 2018;67:2377-2388

54. Boulton AJ, Vinik AI, Arezzo JC, Bril V, Feldman EL, Freeman R, Malik RA, Maser RE, Sosenko JM, Ziegler D, American Diabetes A: Diabetic neuropathies: a statement by the American Diabetes Association. Diabetes Care 2005;28:956-962

55. Salomon C, Scholz-Romero K, Sarker S, Sweeney E, Kobayashi M, Correa P, Longo S, Duncombe G, Mitchell MD, Rice GE, Illanes SE: Gestational Diabetes Mellitus Is Associated With Changes in the Concentration and Bioactivity of Placenta-Derived Exosomes in Maternal Circulation Across Gestation. Diabetes 2016;65:598-609

56. Prattichizzo F, Giuliani A, Sabbatinelli J, Matacchione G, Ramini D, Bonfigli AR, Rippo MR, de Candia P, Procopio AD, Olivieri F, Ceriello A: Prevalence of residual inflammatory risk and associated clinical variables in patients with type 2 diabetes. Diabetes Obes Metab 2020;

57. Togliatto G, Dentelli P, Rosso A, Lombardo G, Gili M, Gallo S, Gai C, Solini A, Camussi G, Brizzi MF: PDGF-BB Carried by Endothelial Cell-Derived Extracellular Vesicles Reduces Vascular Smooth Muscle Cell Apoptosis in Diabetes. Diabetes 2018;67:704-716

58. Xiong Y, Chen L, Yan C, Zhou W, Endo Y, Liu J, Hu L, Hu Y, Mi B, Liu G: Circulating Exosomal miR-20b-5p Inhibition Restores Wnt9b Signaling and Reverses Diabetes-Associated Impaired Wound Healing. Small 2019:e1904044

59. Zampetaki A, Kiechl S, Drozdov I, Willeit P, Mayr U, Prokopi M, Mayr A, Weger S, Oberhollenzer F, Bonora E, Shah A, Willeit J, Mayr M: Plasma microRNA profiling reveals loss of endothelial miR-126 and other microRNAs in type 2 diabetes. Circ Res 2010;107:810-817

60. Fejes Z, Poliska S, Czimmerer Z, Kaplar M, Penyige A, Gal Szabo G, Beke Debreceni I, Kunapuli SP, Kappelmayer J, Nagy B, Jr.: Hyperglycaemia suppresses microRNA expression in platelets to increase P2RY12 and SELP levels in type 2 diabetes mellitus. Thromb Haemost 2017;117:529-542

61. Ryu HS, Park SY, Ma D, Zhang J, Lee W: The induction of microRNA targeting IRS-1 is involved in the development of insulin resistance under conditions of mitochondrial dysfunction in hepatocytes. PLoS One 2011;6:e17343

797 62. Fernandez-Twinn DS, Alfaradhi MZ, Martin-Gronert MS, Duque-Guimaraes DE, Piekarz A, Ferland-
798 McCollough D, Bushell M, Ozanne SE: Downregulation of IRS-1 in adipose tissue of offspring of obese mice
799 is programmed cell-autonomously through post-transcriptional mechanisms. Mol Metab 2014;3:325-333

800 63. Zang J, Maxwell AP, Simpson DA, McKay GJ: Differential Expression of Urinary Exosomal MicroRNAs
801 miR-21-5p and miR-30b-5p in Individuals with Diabetic Kidney Disease. Sci Rep 2019;9:10900
802
803 64. Simonsen JB: Pitfalls associated with lipophilic fluorophore staining of extracellular vesicles for uptake
804 studies. J Extracell Vesicles. 2019 Feb 20;8(1):1582237.
805
806 65. Witwer KW, Buzás EI, Bemis LT, Bora A, Lässer C, Lötvall J, Nolte-'t Hoen EN, Piper MG, Sivaraman
807 S, Skog J, Théry C, Wauben MH, Hochberg F: Standardization of sample collection, isolation and analysis
808 methods in extracellular vesicle research. J Extracell Vesicles. 2013 May 27;2.
809

TABLES

Table 1. Demographic, clinical, and biochemical characteristics of the 218 enrolled subjects. Variables are expressed as mean (standard deviation). P value from ANOVA for continuous variables and from chi squared tests of association for categorical variables. *, p<0.05 vs. CTR; #, p<0.05 vs. T2DM-NC.

Variables	CTR (N=60)	T2DM-NC (N=57)	T2DM-C (N=101)	p-value
Age (years)	66.4 (9.9)	64.4 (9.3)	67.5 (8.0)	0.112
Gender (males)	35	32	71	0.134
BMI (Kg/m^2)	26.0 (4.1)	29.0 (5.1) *	28.5 (4.4) *	<0.001
Waist-hip ratio	0.86 (0.08)	0.93 (0.07) *	0.95 (0.065) *	<0.001
Total cholesterol (mg/dL)	220.6 (41.4)	216.2 (40.1)	197.1 (40.1) *#	0.001
LDL-C (mg/dL)	126.5 (34.8)	129.0 (34.7)	107.9 (30.8) *#	<0.001
HDL-C (mg/dL)	62.8 (16.2)	51.9 (16.0) *	49.5 (12.8) *	<0.001
Triglycerides (mg/dL)	107.98 (82.29)	162.39 (123.90) *	139.65 (95.05)	0.014
Glucose (mg/dL)	95.58 (10.021)	154.72 (50.292) *	176.64 (51.768) *	<0.001
HbA1C (%)	5.913 (0.396)	7.358 (1.149) *	7.768 (1.281) *	<0.001
Insulin (UI/mL)	5.108 (2.941)	10.704 (18.396) *	6.273 (4.789) #	0.006
HOMA index	1.22 (0.71)	4.43 (7.24) *	2.77 (2.32) *#	<0.001
WBC (n/mm^3)	5.99 (1.36)	6.55 (1.81)	6.70 (1.58) *	0.023
Platelets (n/mm^3)	225.1 (50.0)	222.2 (54.0)	214.1 (62.0)	0.447
hs-CRP (mg/L)	2.25 (2.48)	2.70 (2.26)	2.58 (8.81)	0.539
Creatinine (mg/dL)	0.81 (0.17)	0.84 (0.22)	1.04 (0.39) *#	<0.001
Azotemia (mg/dL)	37.3 (8.7)	37.7 (11.5)	44.0 (18.5) *#	0.006
eGFR (mL/min)	83.2 (16.1)	82.9 (22.6)	72.3 (20.7) *#	0.001
Uric acid (mg/dL)	4.60 (1.26)	4.95 (1.46)	4.85 (1.19)	0.305

820

821

Table 2. Binary logistic regression analyses of miRNAs associated with major adverse cardiovascular events (MACE) in T2DM patients **(a)**, and evaluation of the predictive value for MACE of the 4-miRNA model (see Table 3) **(b)** and of the 4-miRNA model after global-mean normalization **(c)** when adjusted for the conventional risk factors. Where applicable, odds ratio (95% CI) are expressed per 0.5 SD increase of each miRNA.

a) 4-miRNA model + risk factors (enter method)				
Variable	**B**	**SE**	**P value**	
4-miRNA signature	9.601	1.753	<0.001	
Age	0.072	0.040	0.073	
Gender (reference category: female)	0.828	0.625	0.185	
Hypertension	0.042	0.683	0.951	
HbA1c	0.354	0.216	0.100	
LDL	0.001	0.008	0.878	
b) 4-miRNA model (global mean normalization) + risk factors (enter method)				
Variable	**B**	**SE**	**P value**	
4-miRNA signature	7.267	1.270	<0.001	
Age	0.060	0.035	0.082	
Gender (reference category: female)	1.135	0.563	0.044	
Hypertension	-0.358	0.597	0.549	
HbA1c	0.435	0.202	0.031	
LDL	-0.003	0.008	0.665	
c) 11-miRNA model (backward method)				
miRNA	**B**	**SE**	**P value**	**OR (95% CI)**
miR-155	-12.749	5.202	0.014	3×10^{-6} (1.084×10^{-10} – 0.078)
miR-195-5p	3.032	1.999	0.129	20.737 (0.412 – 1043.745)
miR-24-3p	-4.039	3.641	0.267	0.018 (1.4×10^{-5} – 22.126)
miR-320a	0.997	0.410	0.015	2.709 (1.213 – 6.054)
miR-342-3p	0.704	0.304	0.021	2.021 (1.113 – 3.670)
miR-376a	0.898	0.371	0.015	2.454 (1.186 – 5.076)
miR-451a	-1.010	0.354	0.004	0.364 (0.182 – 0.728)

FIGURE LEGENDS

Figure 1. Isolation and characterization of CD31$^+$ extracellular vesicles. (A) Schematic representation of the isolation method. (B) Nanoparticle tracking analysis (NTA) of one representative sample of isolated CD31$^+$ EVs, along with the observed mean size and number (from 1 ml of pooled control plasma). (C) Representative TEM image of EVs isolated with CD31 beads along with the relative magnification. (D) Western blot showing the expression of CD31, Alix, TSG101, CD63, ApoB100 and ApoA1 in CD31+ EVs and ultracentrifugation (UC)-collected EVs isolated from the same amount of plasma, along with the relative densitometric analysis. Whole plasma was run as positive control for ApoA1 and ApoB100. (E) Ratio between the expression of CD31 and CD9, CD63, or CD81 in CD31$^+$ EVs vs EVs isolated through UC, as measured with a specific kit allowing cytofluorimetric detection (n=6 from pooled plasma split to perform comparative isolation starting from the same volume). (F) Comparative cytofluorimetric detection of CD49e, CD9, CD63, CD62P, CD81, CD41b, CD42a, CD29, and CD69 in EVs isolated with no beads, scramble IgG beads, and CD31 beads (n=3, from equal amount of control plasma samples). (G) Concentration of collected CD31+ EVs vs the CD31 depleted fraction of EVs subjected to UC, measured with standard NTA (n=3); (H) RT-PCR dosage of miR-126-3p, miR-146a-5p, miR-155, and miR-21-5p in whole plasma vs total EVs isolated with UC vs CD31+EVs, dividing the same control samples in different aliquots (same volume, 100 μl) to compare the relative abundance in the various compartments (n=8). Errors bar are ± SD. *p<0.05, **p<0.01 Student's *t* test for panels D, E, and G; One-way ANOVA for panels F and H.

Figure 2. Comparative concentration, modal size and miRNA profiling of CD31+ EVs from controls and patients with T2DM. NTA measurement of the concentration (A) and modal size (B) of CD31+ EVs isolated from healthy controls and patients with T2DM (n=4); (C) Comparative cytofluorimetric detection of CD31, CD9, CD63, and CD81 of CD31+ EVs isolated from controls

and patients with T2DM (n=4). (D) Heatmap showing miRNAs profiling in CD31^{+}EVs from controls and patients with T2DM (n=5 vs 5, pooled samples). *p<0.05, Student's t test

Figure 3. Expression levels of 11 miRNAs in CD31^{+}EVs from healthy controls, patients with non-complicated T2DM (T2DM-NC) and patients with T2DM and complications (T2DM-C). Violin plots with individual points showing the expression of miR-126-3p, miR-146a-5p, miR-155, miR-195-5p, miR-21-5p, miR-24-3p, miR-320a, miR-342-3p, miR-376a, miR-422, and miR-451a in in a cohort of 218 individuals, 60 healthy (Ctrl), 57 with uncomplicated T2DM (T2DM-NC), and 101 with T2DM and complications (T2DM-C). **p<0.05, ***p<0.01 Kruskal-Wallis followed by Dunn post hoc test.

Figure 4. Diagnostic performance of the differentially expressed miRNAs in CD31^{+}EVs. Receiving operator curves (ROC) and the relative area under the curve (AUC) for differentially expressed miRNAs showing the diagnostic performance for T2DM vs Ctrl (A), T2DM-C vs T2DM-NC (B). ROC curves for miR-146a-5p and miR-21-5p shuttled in CD31+ EVs compared with those of the same miRNAs measured in the same amount of whole plasma with the relative diagnostic performance to detect T2DM vs Ctrl (C) and T2DM-C vs T2DM-NC (D).

Figure 5. Correlations between tested miRNAs and clinical variables and reciprocal among miRNAs. Color-coded correlogram showing the significant Pearson's correlations between tested miRNAs and clinical variables (A) and the reciprocal correlations between miRNAs (B). The intensity of the colour and the dimension of the points depend on the magnitude of the correlation.

Figure 6. *In vitro* treatment of endothelial cells with CD31+ EVs. (A) Schematic representation of the method used to detach EVs from beads; (B) Representative image of endothelial cells treated for 24h with EVs previously stained with a fluorescent green, lipophilic dye (PKH67), and stained

with DAPI to evidence cell nuclei. The relative merge is also shown. (C) Representative image of endothelial cells treated for 24h with EVs previously loaded with a fluorescent (Texas Red), small RNA and stained with DAPI. (D) Relative expression of the non-human *cel-miR-39* in endothelial cells treated with EVs transfected with cel-miR-39 or with the same of amount of the miRNA without EVs (n=3) ***p<0.01 Student's t test. (E) mRNA expression of *CCL2*, *IL-1α*, *TNFα*, *IL-6*, *CXCL-1*, and *CXCL-8* in endothelial cells treated with EVs derived from controls, T2DM-NC, and T2DM-C (n=3) *p<0.05, **p<0.01 One-way ANOVA.

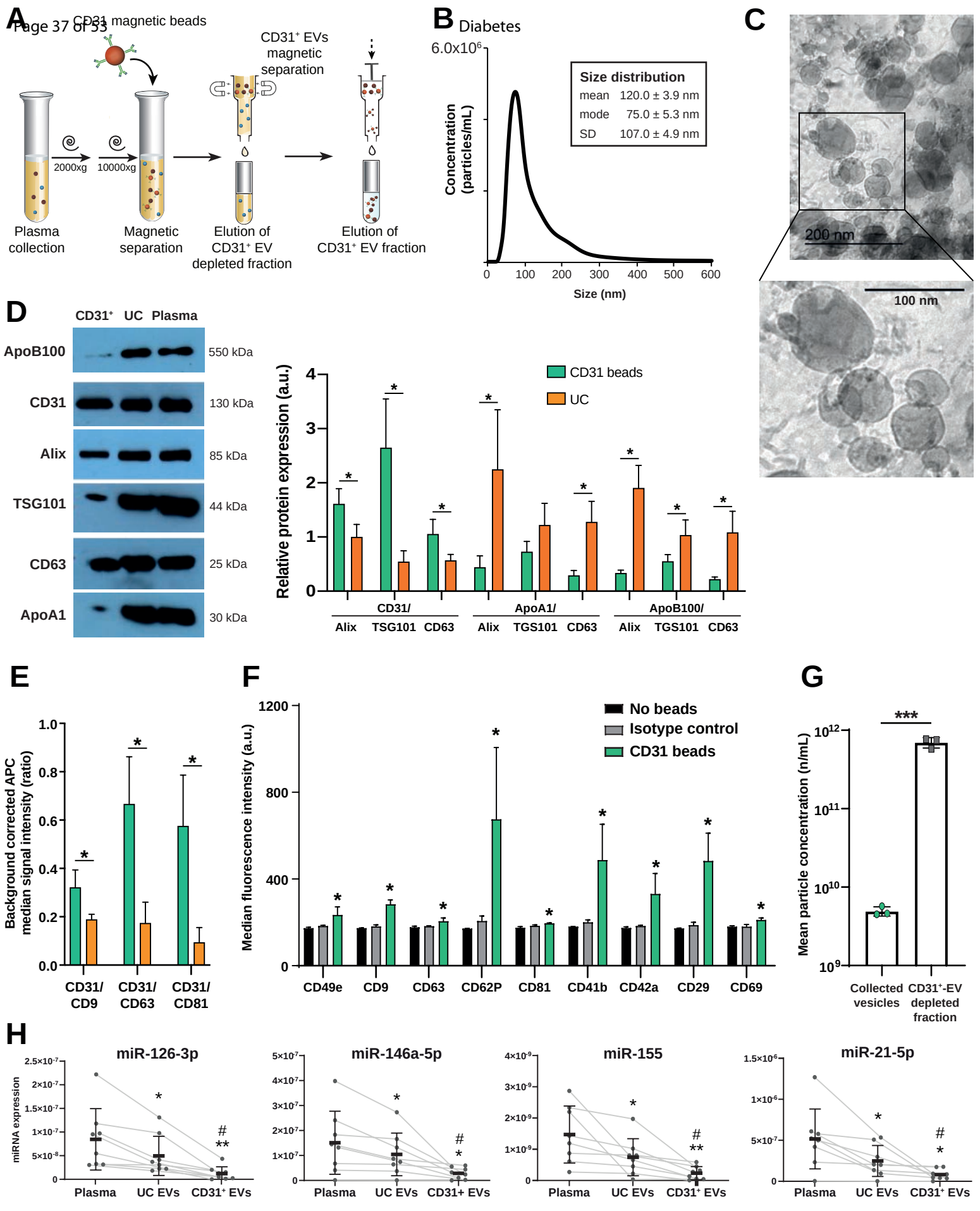
A
CD31 magnetic beads
CD31⁺ EVs magnetic separation
2000xg
10000xg
Plasma collection
Magnetic separation
Elution of CD31⁺ EV depleted fraction
Elution of CD31⁺ EV fraction
B Diabetes
6.0x10⁶
Concentration (particles/mL)
Size distribution
mean 120.0 ± 3.9 nm
mode 75.0 ± 5.3 nm
SD 107.0 ± 4.9 nm
0 100 200 300 400 500 600
Size (nm)
C
200 nm
100 nm
D
CD31⁺ UC Plasma
ApoB100 550 kDa
CD31 130 kDa
Alix 85 kDa
TSG101 44 kDa
CD63 25 kDa
ApoA1 30 kDa
Relative protein expression (a.u.)
CD31 beads
UC
CD31/ Alix TSG101 CD63
ApoA1/ Alix TGS101 CD63
ApoB100/ Alix TGS101 CD63
E
Background corrected APC median signal intensity (ratio)
CD31/ CD9
CD31/ CD63
CD31/ CD81
F
Median fluorescence intensity (a.u.)
No beads
Isotype control
CD31 beads
CD49e CD9 CD63 CD62P CD81 CD41b CD42a CD29 CD69
G
Mean particle concentration (n/mL)
***
Collected vesicles
CD31⁺-EV depleted fraction
H
miR-126-3p
miR-146a-5p
miR-155
miR-21-5p
miRNA expression
Plasma UC EVs CD31⁺ EVs
Plasma UC EVs CD31+ EVs

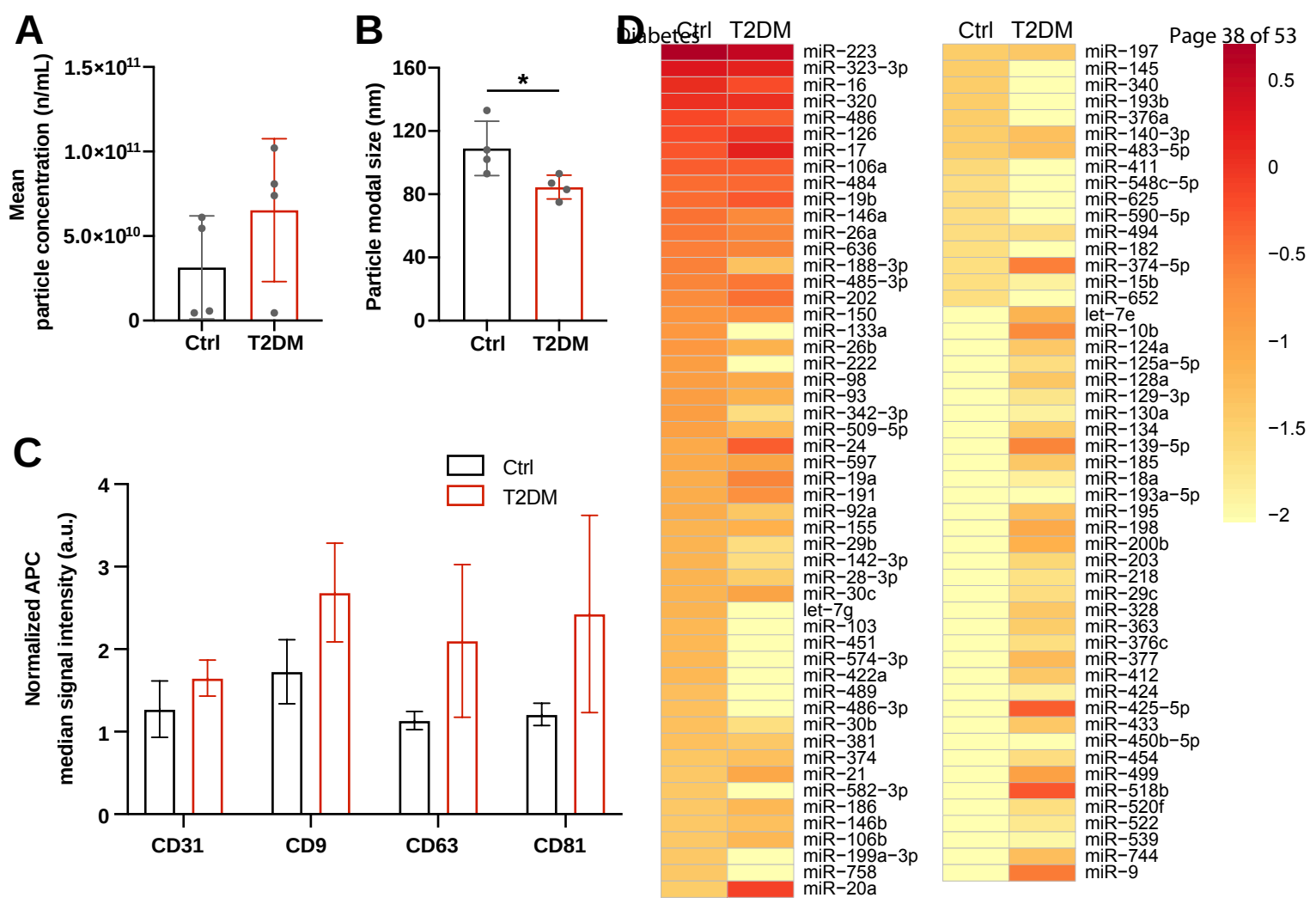
A
Mean particle concentration (n/mL)
1.5×10^11
1.0×10^11
5.0×10^10
0
Ctrl
T2DM
B
Particle modal size (nm)
160
120
80
40
0
*
Ctrl
T2DM
C
Normalized APC median signal intensity (a.u.)
Ctrl
T2DM
4
3
2
1
0
CD31
CD9
CD63
CD81
D
Ctrl
T2DM
miR-223
miR-323-3p
miR-16
miR-320
miR-486
miR-126
miR-17
miR-106a
miR-484
miR-19b
miR-146a
miR-26a
miR-636
miR-188-3p
miR-485-3p
miR-202
miR-150
miR-133a
miR-26b
miR-222
miR-98
miR-93
miR-342-3p
miR-509-5p
miR-24
miR-597
miR-19a
miR-191
miR-92a
miR-155
miR-29b
miR-142-3p
miR-28-3p
miR-30c
let-7g
miR-103
miR-451
miR-574-3p
miR-422a
miR-489
miR-486-3p
miR-30b
miR-381
miR-374
miR-21
miR-582-3p
miR-186
miR-146b
miR-106b
miR-199a-3p
miR-758
miR-20a
Ctrl
T2DM
miR-197
miR-145
miR-340
miR-193b
miR-376a
miR-140-3p
miR-483-5p
miR-411
miR-548c-5p
miR-625
miR-590-5p
miR-494
miR-182
miR-374-5p
miR-15b
miR-652
let-7e
miR-10b
miR-124a
miR-125a-5p
miR-128a
miR-129-3p
miR-130a
miR-134
miR-139-5p
miR-185
miR-18a
miR-193a-5p
miR-195
miR-198
miR-200b
miR-203
miR-218
miR-29c
miR-328
miR-363
miR-376c
miR-377
miR-412
miR-424
miR-425-5p
miR-433
miR-450b-5p
miR-454
miR-499
miR-518b
miR-520f
miR-522
miR-539
miR-744
miR-9
0.5
0
−0.5
−1
−1.5
−2

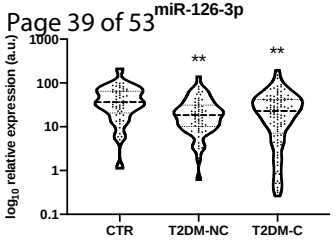
miR-126-3p
log10 relative expression (a.u.)
CTR
T2DM-NC
T2DM-C

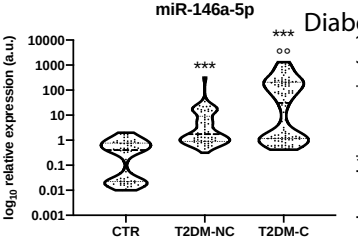
miR-146a-5p
log10 relative expression (a.u.)
CTR
T2DM-NC
T2DM-C

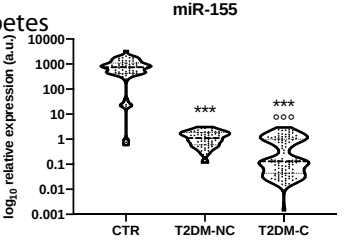
miR-155
log10 relative expression (a.u.)
CTR
T2DM-NC
T2DM-C

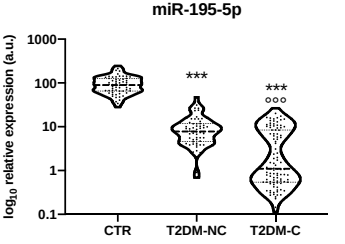
miR-195-5p
log10 relative expression (a.u.)
CTR
T2DM-NC
T2DM-C

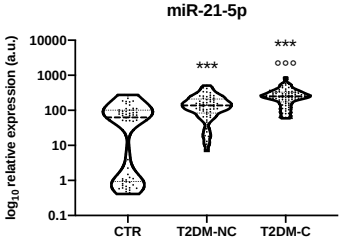
miR-21-5p
log10 relative expression (a.u.)
CTR
T2DM-NC
T2DM-C

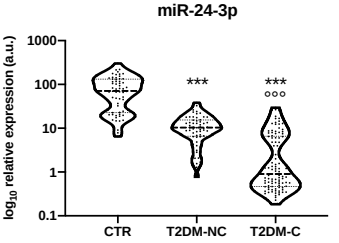
miR-24-3p
log10 relative expression (a.u.)
CTR
T2DM-NC
T2DM-C

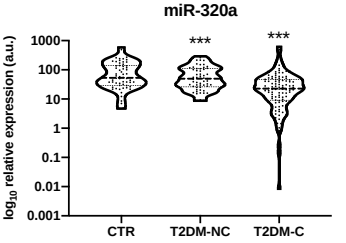
miR-320a
log10 relative expression (a.u.)
CTR
T2DM-NC
T2DM-C

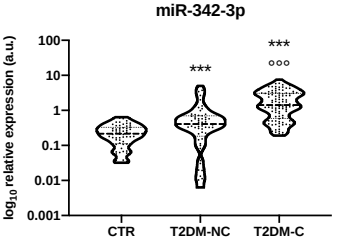
miR-342-3p
log10 relative expression (a.u.)
CTR
T2DM-NC
T2DM-C

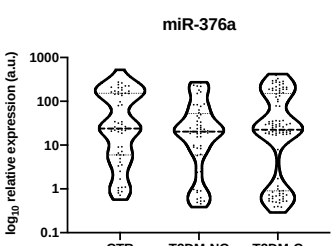
miR-376a
log10 relative expression (a.u.)
CTR
T2DM-NC
T2DM-C

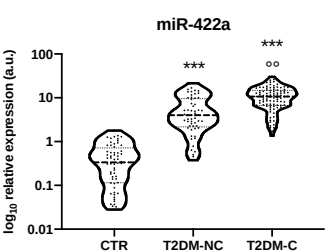
miR-422a
log10 relative expression (a.u.)
CTR
T2DM-NC
T2DM-C

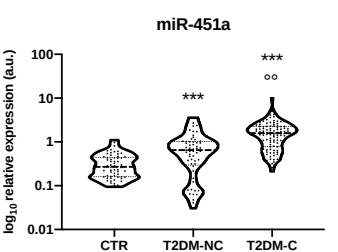
miR-451a
log10 relative expression (a.u.)
CTR
T2DM-NC
T2DM-C

A

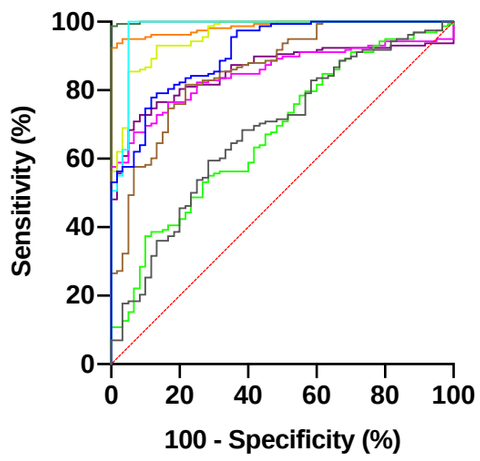

	AUC	p value
miR-126-3p	0.679	<0.0001
miR-146a-5p	0.911	<0.0001
miR-155	0.978	<0.0001
miR-195-5p	0.999	<0.0001
miR-21-5p	0.859	<0.0001
miR-24-3p	0.960	<0.0001
miR-320a	0.673	<0.0001
miR-342-3p	0.850	<0.0001
miR-422a	0.985	<0.0001
miR-451a	0.857	<0.0001

B

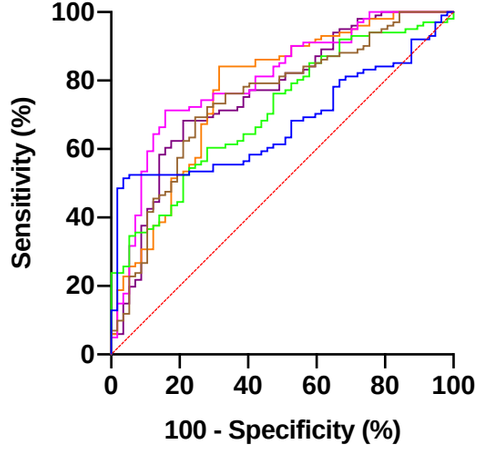

	AUC	p value
miR-146a-5p	0.673	0.0003
miR-21-5p	0.744	<0.0001
miR-320a	0.709	<0.0001
miR-342-3p	0.801	<0.0001
miR-422a	0.770	<0.0001
miR-451a	0.769	<0.0001

C

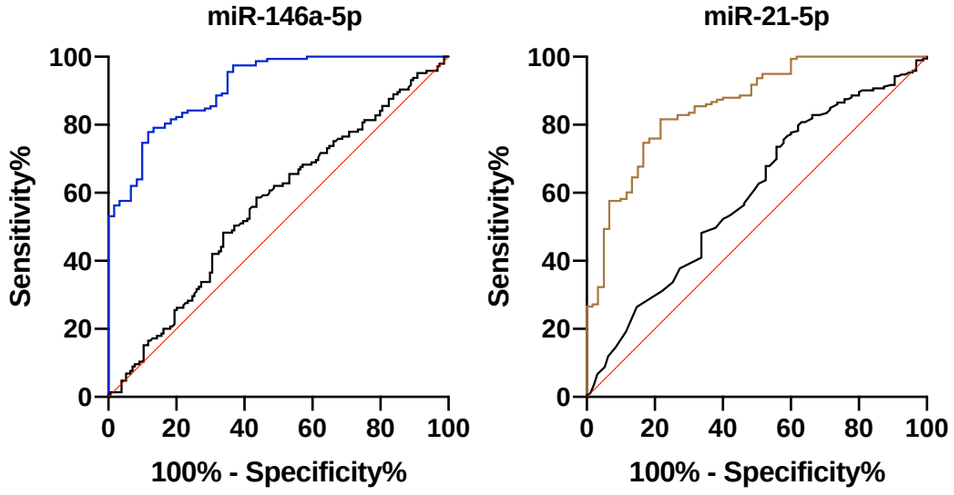

	AUC	p value
miR-146a-5p		
Plasma	0.562	0.064
CD31$^+$EVs	0.911	<0.0001
miR-21-5p		
Plasma	0.595	0.009
CD31$^+$EVs	0.859	<0.0001

D

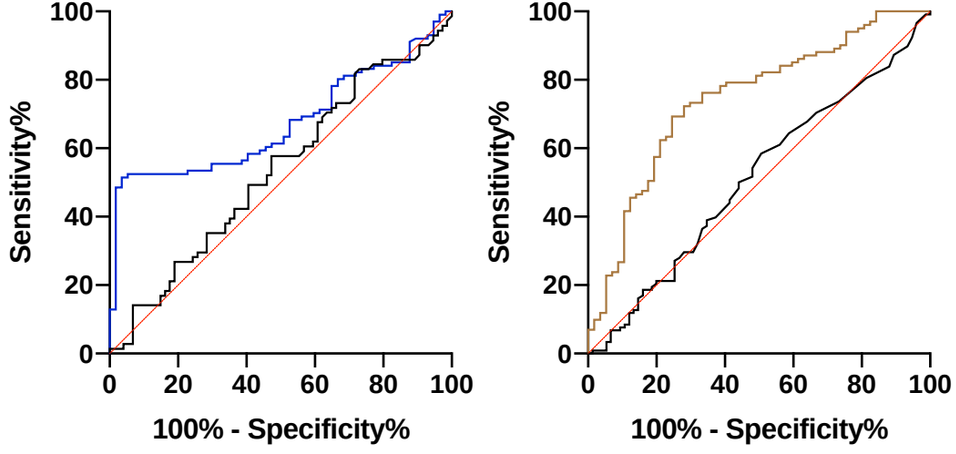

	AUC	p value
miR-146a-5p		
Plasma	0.533	0.496
CD31$^+$EVs	0.673	<0.001
miR-21-5p		
Plasma	0.511	0.798
CD31$^+$EVs	0.744	<0.0001

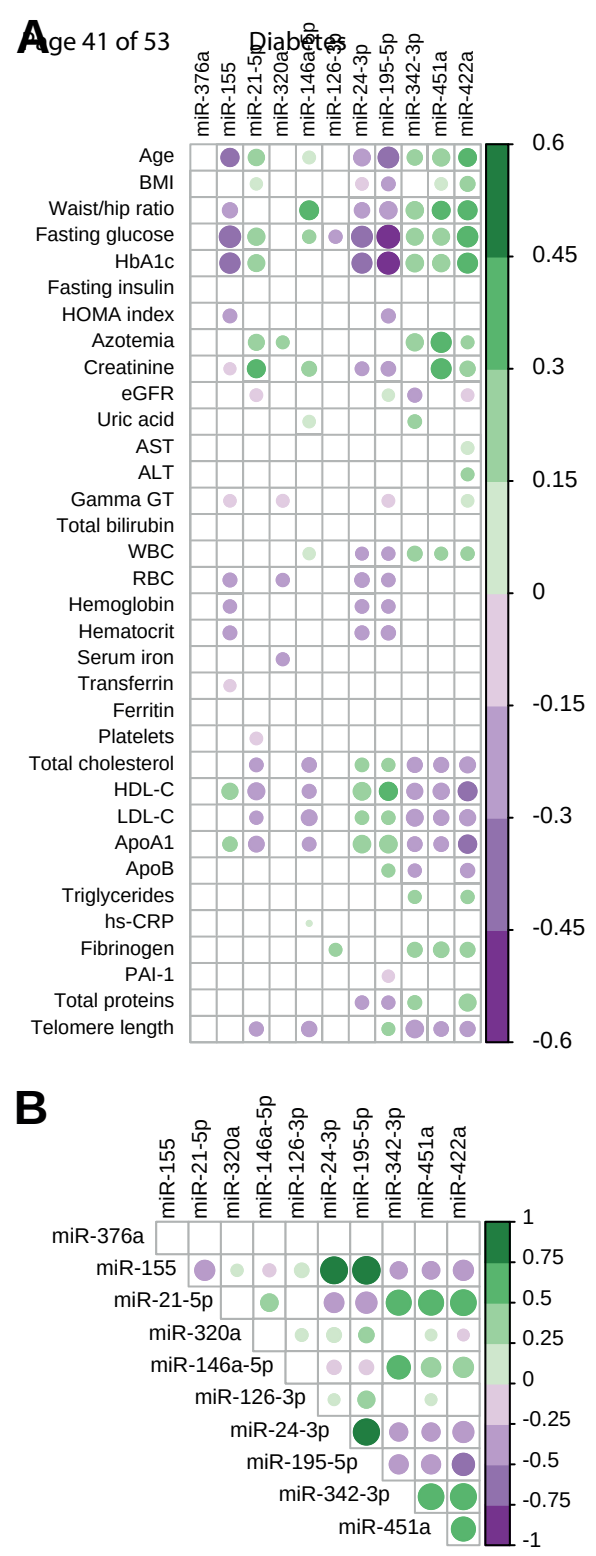
A
miR-376a
miR-155
miR-21-5p
miR-320a
miR-146a-5p
miR-126-3p
miR-24-3p
miR-195-5p
miR-342-3p
miR-451a
miR-422a
Age
BMI
Waist/hip ratio
Fasting glucose
HbA1c
Fasting insulin
HOMA index
Azotemia
Creatinine
eGFR
Uric acid
AST
ALT
Gamma GT
Total bilirubin
WBC
RBC
Hemoglobin
Hematocrit
Serum iron
Transferrin
Ferritin
Platelets
Total cholesterol
HDL-C
LDL-C
ApoA1
ApoB
Triglycerides
hs-CRP
Fibrinogen
PAI-1
Total proteins
Telomere length
0.6
0.45
0.3
0.15
0
-0.15
-0.3
-0.45
-0.6
B
miR-155
miR-21-5p
miR-320a
miR-146a-5p
miR-126-3p
miR-24-3p
miR-195-5p
miR-342-3p
miR-451a
miR-422a
miR-376a
miR-155
miR-21-5p
miR-320a
miR-146a-5p
miR-126-3p
miR-24-3p
miR-195-5p
miR-342-3p
miR-451a
1
0.75
0.5
0.25
0
-0.25
-0.5
-0.75
-1

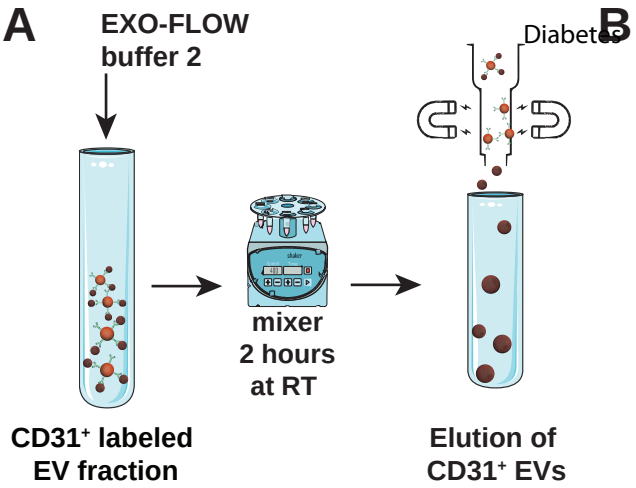
A
EXO-FLOW
buffer 2
mixer
2 hours
at RT
CD31⁺ labeled
EV fraction
Elution of
CD31⁺ EVs

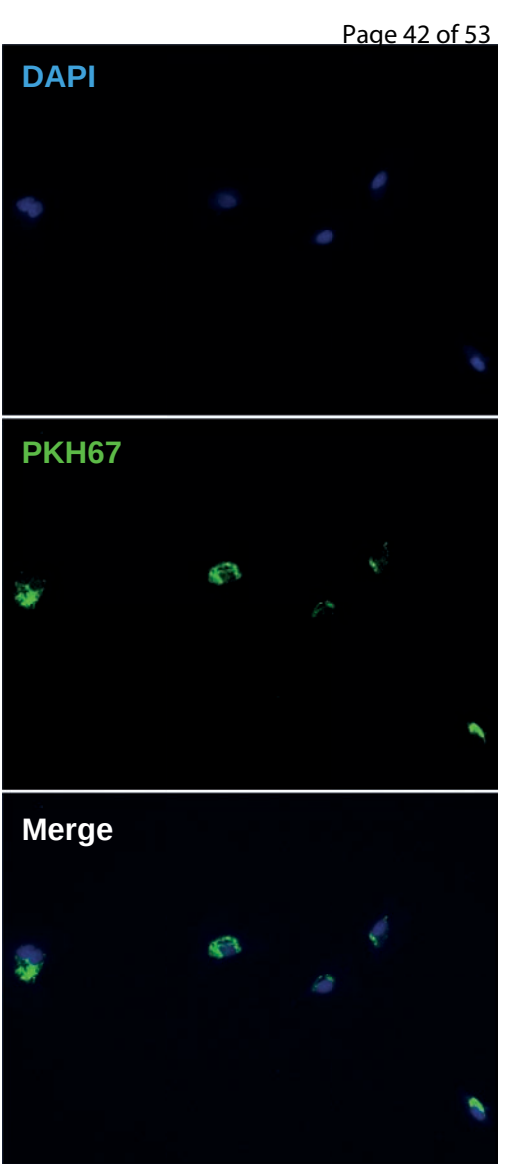
B
DAPI
PKH67
Merge

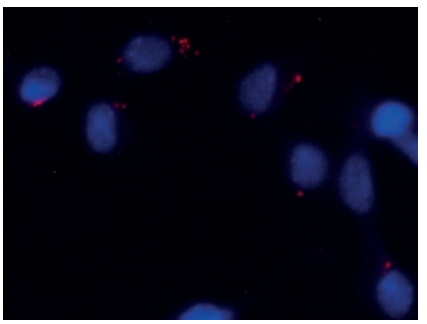
C

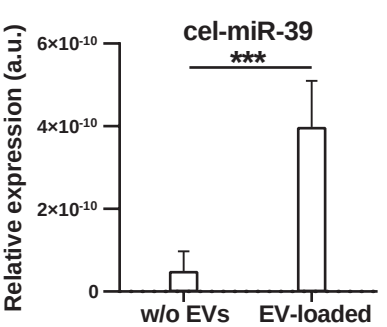
D
cel-miR-39
***
Relative expression (a.u.)
6×10-10
4×10-10
2×10-10
0
w/o EVs
EV-loaded

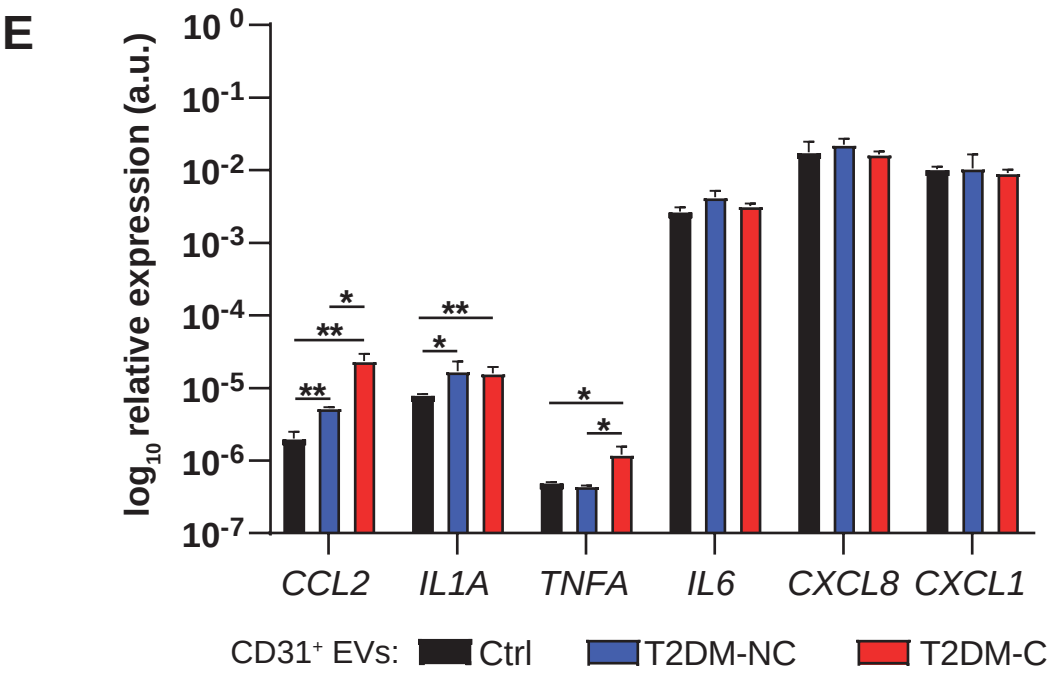
E
log10 relative expression (a.u.)
10 0
10-1
10-2
10-3
10-4
10-5
10-6
10-7
CCL2
IL1A
TNFA
IL6
CXCL8
CXCL1
CD31⁺ EVs:
Ctrl
T2DM-NC
T2DM-C

Supplementary Figure 1

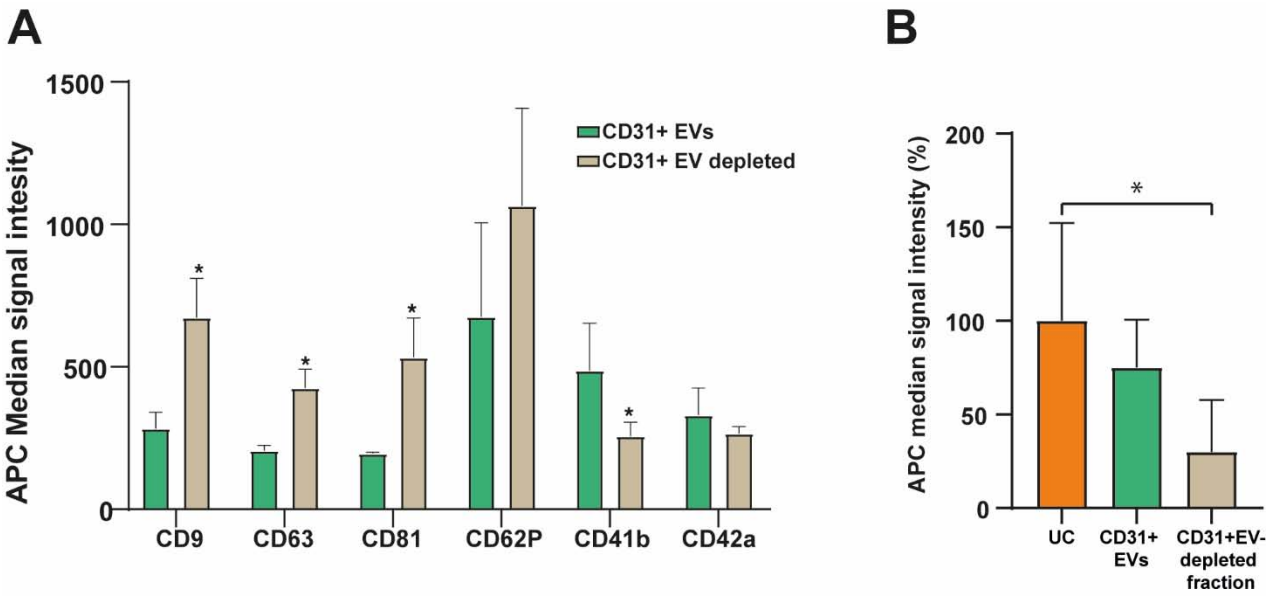

A) Comparative cytofluorimetric detection of multiple markers in CD31+EVs vs CD31+ EV-depleted (n=3, from the same control plasma samples). * t test $p<0.05$. **B)** Estimation of the yield of the isolation technique. Comparative cytofluorimetric detection of CD31 in EVs isolated with UC, in CD31+EVs, and the CD31+ depleted EVs (n=3, from the same control plasma samples). * ANOVA $p<0.05$.

Supplementary Table 1. Literature supporting the selection of the miRNA panel.

miRNA	References
miR-126-3p	(Al-Kafaji et al., 2017; Amr et al., 2018; Jansen et al., 2016; Jansen et al., 2013; Liu et al., 2014; Meng et al., 2012; Mocharla et al., 2013; Olivieri et al., 2014; Olivieri et al., 2015b; Ortega et al., 2014; Rawal et al., 2017; Seyhan et al., 2016; Wang et al., 2014; Zampetaki et al., 2010; Zhang et al., 2017; Zhang et al., 2015; Zhang et al., 2013)
miR-146a-5p	(Alipoor et al., 2017; Baldeon et al., 2014; Garcia-Jacobo et al., 2019; Kong et al., 2011; Mensa et al., 2019; Radovic et al., 2018; Rong et al., 2013)
miR-155	(Akhbari et al., 2019; Barutta et al., 2013; Beltrami et al., 2018; CorralFernandez et al., 2013; Huang et al., 2014; Liang et al., 2018a; Liang et al., 2018b; Mazloom et al., 2015; Moura et al., 2019; Tome-Carneiro et al., 2013; Wang et al., 2019; Wang et al., 2018; Yang et al., 2015)
miR-195-5p	(Marques et al., 2016)
miR-21-5p	(Chien et al., 2016; Ghorbani et al., 2018; Jansen et al., 2016; Jiang et al., 2017; La Sala et al., 2019; Liang et al., 2018b; Nunez Lopez et al., 2016; Olivieri et al., 2015a; Villard et al., 2015; Wang et al., 2014; Zampetaki et al., 2010; Zang et al., 2019)
miR-24-3p	(de Candia et al., 2017; Demirsoy et al., 2018; Kokkinopoulou et al., 2019; Prabu et al., 2019)
miR-320a	(Flowers et al., 2015; Villard et al., 2015)
miR-342-3p	(Assmann et al., 2018; Collares et al., 2013; de Candia et al., 2017)
miR-376a	(Joglekar et al., 2009)
miR-422a	(Latorre et al., 2017)
miR-451a	(Ding et al., 2016)

Akhbari, M., Khalili, M., Shahrabi-Farahani, M., Biglari, A., Bandarian, F., 2019. Expression Level of Circulating Cell Free miR-155 Gene in Serum of Patients with Diabetic Nephropathy. Clin Lab 65.

Al-Kafaji, G., Al-Mahroos, G., Abdulla Al-Muhtaresh, H., Sabry, M.A., Abdul Razzak, R., Salem, A.H., 2017. Circulating endothelium-enriched microRNA-126 as a potential biomarker for coronary artery disease in type 2 diabetes mellitus patients. Biomarkers 22, 268-278.

Alipoor, B., Ghaedi, H., Meshkani, R., Torkamandi, S., Saffari, S., Iranpour, M., Omrani, M.D., 2017. Association of MiR-146a Expression and Type 2 Diabetes Mellitus: A Meta-Analysis. Int J Mol Cell Med 6, 156-163.

Amr, K.S., Abdelmawgoud, H., Ali, Z.Y., Shehata, S., Raslan, H.M., 2018. Potential value of circulating microRNA126 and microRNA-210 as biomarkers for type 2 diabetes with coronary artery disease. Br J Biomed Sci 75, 82-87.

Assmann, T.S., Recamonde-Mendoza, M., de Souza, B.M., Bauer, A.C., Crispim, D., 2018. MicroRNAs and diabetic kidney disease: Systematic review and bioinformatic analysis. Mol Cell Endocrinol 477, 90-102.

Baldeon, R.L., Weigelt, K., de Wit, H., Ozcan, B., van Oudenaren, A., Sempertegui, F., Sijbrands, E., Grosse, L., Freire, W., Drexhage, H.A., Leenen, P.J., 2014. Decreased serum level of miR-146a as sign of chronic inflammation in type 2 diabetic patients. PLoS One 9, e115209.

Barutta, F., Tricarico, M., Corbelli, A., Annaratone, L., Pinach, S., Grimaldi, S., Bruno, G., Cimino, D., Taverna, D., Deregibus, M.C., Rastaldi, M.P., Perin, P.C., Gruden, G., 2013. Urinary exosomal microRNAs in incipient diabetic nephropathy. PLoS One 8, e73798.

Beltrami, C., Simpson, K., Jesky, M., Wonnacott, A., Carrington, C., Holmans, P., Newbury, L., Jenkins, R., Ashdown, T., Dayan, C., Satchell, S., Corish, P., Cockwell, P., Fraser, D., Bowen, T., 2018. Association of Elevated Urinary miR-126, miR-155, and miR-29b with Diabetic Kidney Disease. Am J Pathol 188, 1982-1992.

Chien, H.Y., Chen, C.Y., Chiu, Y.H., Lin, Y.C., Li, W.C., 2016. Differential microRNA Profiles Predict Diabetic Nephropathy Progression in Taiwan. Int J Med Sci 13, 457-465.

Collares, C.V., Evangelista, A.F., Xavier, D.J., Rassi, D.M., Arns, T., Foss-Freitas, M.C., Foss, M.C., Puthier, D., Sakamoto-Hojo, E.T., Passos, G.A., Donadi, E.A., 2013. Identifying common and specific microRNAs expressed in peripheral blood mononuclear cell of type 1, type 2, and gestational diabetes mellitus patients. BMC Res Notes 6, 491.

Corral-Fernandez, N.E., Salgado-Bustamante, M., Martinez-Leija, M.E., Cortez-Espinosa, N., Garcia-Hernandez, M.H., Reynaga-Hernandez, E., Quezada-Calvillo, R., Portales-Perez, D.P., 2013. Dysregulated miR-155 expression in peripheral blood mononuclear cells from patients with type 2 diabetes. Exp Clin Endocrinol Diabetes 121, 347-353.

de Candia, P., Spinetti, G., Specchia, C., Sangalli, E., La Sala, L., Uccellatore, A., Lupini, S., Genovese, S., Matarese, G., Ceriello, A., 2017. A unique plasma microRNA profile defines type 2 diabetes progression. PLoS One 12, e0188980.

Demirsoy, I.H., Ertural, D.Y., Balci, S., Cinkir, U., Sezer, K., Tamer, L., Aras, N., 2018. Profiles of Circulating MiRNAs Following Metformin Treatment in Patients with Type 2 Diabetes. J Med Biochem 37, 499-506.

Ding, L., Ai, D., Wu, R., Zhang, T., Jing, L., Lu, J., Zhong, L., 2016. Identification of the differential expression of serum microRNA in type 2 diabetes. Biosci Biotechnol Biochem 80, 461-465.

Flowers, E., Aouizerat, B.E., Abbasi, F., Lamendola, C., Grove, K.M., Fukuoka, Y., Reaven, G.M., 2015. Circulating microRNA-320a and microRNA-486 predict thiazolidinedione response: Moving towards precision health for diabetes prevention. Metabolism 64, 1051-1059.

Garcia-Jacobo, R.E., Uresti-Rivera, E.E., Portales-Perez, D.P., Gonzalez-Amaro, R., Lara-Ramirez, E.E., EncisoMoreno, J.A., Garcia-Hernandez, M.H., 2019. Circulating miR-146a, miR-34a and miR-375 in type 2 diabetes patients, pre-diabetic and normal-glycaemic individuals in relation to beta-cell function, insulin resistance and metabolic parameters. Clin Exp Pharmacol Physiol 46, 1092-1100.

Ghorbani, S., Mahdavi, R., Alipoor, B., Panahi, G., Nasli Esfahani, E., Razi, F., Taghikhani, M., Meshkani, R., 2018. Decreased serum microRNA-21 level is associated with obesity in healthy and type 2 diabetic subjects. Arch Physiol Biochem 124, 300-305.

Huang, Y., Liu, Y., Li, L., Su, B., Yang, L., Fan, W., Yin, Q., Chen, L., Cui, T., Zhang, J., Lu, Y., Cheng, J., Fu, P., Liu, F., 2014. Involvement of inflammation-related miR-155 and miR-146a in diabetic nephropathy: implications for glomerular endothelial injury. BMC Nephrol 15, 142.

Jansen, F., Wang, H., Przybilla, D., Franklin, B.S., Dolf, A., Pfeifer, P., Schmitz, T., Flender, A., Endl, E., Nickenig, G., Werner, N., 2016. Vascular endothelial microparticles-incorporated microRNAs are altered in patients with diabetes mellitus. Cardiovasc Diabetol 15, 49.

Jansen, F., Yang, X., Hoelscher, M., Cattelan, A., Schmitz, T., Proebsting, S., Wenzel, D., Vosen, S., Franklin, B.S., Fleischmann, B.K., Nickenig, G., Werner, N., 2013. Endothelial microparticle-mediated transfer of MicroRNA-126 promotes vascular endothelial cell repair via SPRED1 and is abrogated in glucose-damaged endothelial microparticles. Circulation 128, 2026-2038.

Jiang, Q., Lyu, X.M., Yuan, Y., Wang, L., 2017. Plasma miR-21 expression: an indicator for the severity of Type 2 diabetes with diabetic retinopathy. Biosci Rep 37.

Joglekar, M.V., Joglekar, V.M., Hardikar, A.A., 2009. Expression of islet-specific microRNAs during human pancreatic development. Gene Expr Patterns 9, 109-113.

Kokkinopoulou, I., Maratou, E., Mitrou, P., Boutati, E., Sideris, D.C., Fragoulis, E.G., Christodoulou, M.I., 2019. Decreased expression of microRNAs targeting type-2 diabetes susceptibility genes in peripheral blood of patients and predisposed individuals. Endocrine 66, 226-239.

Kong, L., Zhu, J., Han, W., Jiang, X., Xu, M., Zhao, Y., Dong, Q., Pang, Z., Guan, Q., Gao, L., Zhao, J., Zhao, L., 2011. Significance of serum microRNAs in pre-diabetes and newly diagnosed type 2 diabetes: a clinical study. Acta Diabetol 48, 61-69.

La Sala, L., Mrakic-Sposta, S., Tagliabue, E., Prattichizzo, F., Micheloni, S., Sangalli, E., Specchia, C., Uccellatore, A.C., Lupini, S., Spinetti, G., de Candia, P., Ceriello, A., 2019. Circulating microRNA-21 is an early predictor of ROS-mediated damage in subjects with high risk of developing diabetes and in drug-naive T2D. Cardiovasc Diabetol 18, 18.

Latorre, J., Moreno-Navarrete, J.M., Mercader, J.M., Sabater, M., Rovira, O., Girones, J., Ricart, W., Fernandez-Real, J.M., Ortega, F.J., 2017. Decreased lipid metabolism but increased FA biosynthesis are coupled with changes in liver microRNAs in obese subjects with NAFLD. Int J Obes (Lond) 41, 620-630.

Liang, Y.Z., Dong, J., Zhang, J., Wang, S., He, Y., Yan, Y.X., 2018a. Identification of Neuroendocrine Stress Response-Related Circulating MicroRNAs as Biomarkers for Type 2 Diabetes Mellitus and Insulin Resistance. Front Endocrinol (Lausanne) 9, 132.

Liang, Y.Z., Li, J.J., Xiao, H.B., He, Y., Zhang, L., Yan, Y.X., 2018b. Identification of stress-related microRNA biomarkers in type 2 diabetes mellitus: A systematic review and meta-analysis. J Diabetes.

Liu, Y., Gao, G., Yang, C., Zhou, K., Shen, B., Liang, H., Jiang, X., 2014. The role of circulating microRNA-126 (miR126): a novel biomarker for screening prediabetes and newly diagnosed type 2 diabetes mellitus. Int J Mol Sci 15, 10567-10577.

Marques, F.Z., Vizi, D., Khammy, O., Mariani, J.A., Kaye, D.M., 2016. The transcardiac gradient of cardiomicroRNAs in the failing heart. Eur J Heart Fail 18, 1000-1008.

Mazloom, H., Alizadeh, S., Pasalar, P., Esfahani, E.N., Meshkani, R., 2015. Downregulated microRNA-155 expression in peripheral blood mononuclear cells of type 2 diabetic patients is not correlated with increased inflammatory cytokine production. Cytokine 76, 403-408.

Meng, S., Cao, J.T., Zhang, B., Zhou, Q., Shen, C.X., Wang, C.Q., 2012. Downregulation of microRNA-126 in endothelial progenitor cells from diabetes patients, impairs their functional properties, via target gene Spred-1. J Mol Cell Cardiol 53, 64-72.

Mensa, E., Giuliani, A., Matacchione, G., Gurau, F., Bonfigli, A.R., Romagnoli, F., De Luca, M., Sabbatinelli, J., Olivieri, F., 2019. Circulating miR-146a in healthy aging and type 2 diabetes: Age- and gender-specific trajectories. Mech Ageing Dev 180, 1-10.

Mocharla, P., Briand, S., Giannotti, G., Dorries, C., Jakob, P., Paneni, F., Luscher, T., Landmesser, U., 2013. AngiomiR-126 expression and secretion from circulating CD34(+) and CD14(+) PBMCs: role for proangiogenic effects and alterations in type 2 diabetics. Blood 121, 226-236.

Moura, J., Sorensen, A., Leal, E.C., Svendsen, R., Carvalho, L., Willemoes, R.J., Jorgensen, P.T., Jenssen, H., Wengel, J., Dalgaard, L.T., Carvalho, E., 2019. microRNA-155 inhibition restores Fibroblast Growth Factor 7 expression in diabetic skin and decreases wound inflammation. Sci Rep 9, 5836.

Nunez Lopez, Y.O., Garufi, G., Seyhan, A.A., 2016. Altered levels of circulating cytokines and microRNAs in lean and obese individuals with prediabetes and type 2 diabetes. Mol Biosyst 13, 106-121.

Olivieri, F., Bonafe, M., Spazzafumo, L., Gobbi, M., Prattichizzo, F., Recchioni, R., Marcheselli, F., La Sala, L., Galeazzi, R., Rippo, M.R., Fulgenzi, G., Angelini, S., Lazzarini, R., Bonfigli, A.R., Bruge, F., Tiano, L., Genovese, S., Ceriello, A., Boemi, M., Franceschi, C., Procopio, A.D., Testa, R., 2014. Age- and glycemiarelated miR-126-3p levels in plasma and endothelial cells. Aging (Albany NY) 6, 771-787.

Olivieri, F., Spazzafumo, L., Bonafe, M., Recchioni, R., Prattichizzo, F., Marcheselli, F., Micolucci, L., Mensa, E., Giuliani, A., Santini, G., Gobbi, M., Lazzarini, R., Boemi, M., Testa, R., Antonicelli, R., Procopio, A.D., Bonfigli, A.R., 2015a. MiR-21-5p and miR-126a-3p levels in plasma and circulating angiogenic cells: relationship with type 2 diabetes complications. Oncotarget 6, 35372-35382.

Olivieri, F., Spazzafumo, L., Bonafè, M., Recchioni, R., Prattichizzo, F., Marcheselli, F., Micolucci, L., Mensà, E., Giuliani, A., Santini, G., Gobbi, M., Lazzarini, R., Boemi, M., Testa, R., Antonicelli, R., Procopio, A.D., Bonfigli, A.R., 2015b. MiR-21-5p and miR-126a-3p levels in plasma and circulating angiogenic cells: Relationship with type 2 diabetes complications. Oncotarget 6, 35372-35382.

Ortega, F.J., Mercader, J.M., Moreno-Navarrete, J.M., Rovira, O., Guerra, E., Esteve, E., Xifra, G., Martinez, C., Ricart, W., Rieusset, J., Rome, S., Karczewska-Kupczewska, M., Straczkowski, M., Fernandez-Real, J.M., 2014. Profiling of circulating microRNAs reveals common microRNAs linked to type 2 diabetes that change with insulin sensitization. Diabetes Care 37, 1375-1383.

Prabu, P., Rome, S., Sathishkumar, C., Gastebois, C., Meugnier, E., Mohan, V., Balasubramanyam, M., 2019. MicroRNAs from urinary extracellular vesicles are non-invasive early biomarkers of diabetic nephropathy in type 2 diabetes patients with the 'Asian Indian phenotype'. Diabetes Metab 45, 276-285.

Radovic, N., Nikolic Jakoba, N., Petrovic, N., Milosavljevic, A., Brkovic, B., Roganovic, J., 2018. MicroRNA-146a and microRNA-155 as novel crevicular fluid biomarkers for periodontitis in non-diabetic and type 2 diabetic patients. J Clin Periodontol 45, 663-671.

Rawal, S., Munasinghe, P.E., Shindikar, A., Paulin, J., Cameron, V., Manning, P., Williams, M.J., Jones, G.T., Bunton, R., Galvin, I., Katare, R., 2017. Down-regulation of proangiogenic microRNA-126 and microRNA-132 are early modulators of diabetic cardiac microangiopathy. Cardiovasc Res 113, 90-101.

Rong, Y., Bao, W., Shan, Z., Liu, J., Yu, X., Xia, S., Gao, H., Wang, X., Yao, P., Hu, F.B., Liu, L., 2013. Increased microRNA-146a levels in plasma of patients with newly diagnosed type 2 diabetes mellitus. PLoS One 8, e73272.

Seyhan, A.A., Nunez Lopez, Y.O., Xie, H., Yi, F., Mathews, C., Pasarica, M., Pratley, R.E., 2016. Pancreas-enriched miRNAs are altered in the circulation of subjects with diabetes: a pilot cross-sectional study. Sci Rep 6, 31479.

Tome-Carneiro, J., Larrosa, M., Yanez-Gascon, M.J., Davalos, A., Gil-Zamorano, J., Gonzalvez, M., Garcia-Almagro, F.J., Ruiz Ros, J.A., Tomas-Barberan, F.A., Espin, J.C., Garcia-Conesa, M.T., 2013. One-year supplementation with a grape extract containing resveratrol modulates inflammatory-related microRNAs and cytokines expression in peripheral blood mononuclear cells of type 2 diabetes and hypertensive patients with coronary artery disease. Pharmacol Res 72, 69-82.

Villard, A., Marchand, L., Thivolet, C., Rome, S., 2015. Diagnostic Value of Cell-free Circulating MicroRNAs for Obesity and Type 2 Diabetes: A Meta-analysis. J Mol Biomark Diagn 6.

Wang, J., Wang, G., Liang, Y., Zhou, X., 2019. Expression Profiling and Clinical Significance of Plasma MicroRNAs in Diabetic Nephropathy. J Diabetes Res 2019, 5204394.

Wang, X., Sundquist, J., Zoller, B., Memon, A.A., Palmer, K., Sundquist, K., Bennet, L., 2014. Determination of 14 circulating microRNAs in Swedes and Iraqis with and without diabetes mellitus type 2. PLoS One 9, e86792.

Wang, Y., Zheng, Z.J., Jia, Y.J., Yang, Y.L., Xue, Y.M., 2018. Role of p53/miR-155-5p/sirt1 loop in renal tubular injury of diabetic kidney disease. J Transl Med 16, 146.

Yang, T.T., Song, S.J., Xue, H.B., Shi, D.F., Liu, C.M., Liu, H., 2015. Regulatory T cells in the pathogenesis of type 2 diabetes mellitus retinopathy by miR-155. Eur Rev Med Pharmacol Sci 19, 2010-2015.

Zampetaki, A., Kiechl, S., Drozdov, I., Willeit, P., Mayr, U., Prokopi, M., Mayr, A., Weger, S., Oberhollenzer, F., Bonora, E., Shah, A., Willeit, J., Mayr, M., 2010. Plasma microRNA profiling reveals loss of endothelial miR126 and other microRNAs in type 2 diabetes. Circ Res 107, 810-817.

Zang, J., Maxwell, A.P., Simpson, D.A., McKay, G.J., 2019. Differential Expression of Urinary Exosomal MicroRNAs miR-21-5p and miR-30b-5p in Individuals with Diabetic Kidney Disease. Sci Rep 9, 10900.

Zhang, J., Sun, X.J., Chen, J., Hu, Z.W., Wang, L., Gu, D.M., Wang, A.P., 2017. Increasing the miR-126 expression in the peripheral blood of patients with diabetic foot ulcers treated with maggot debridement therapy. J Diabetes Complications 31, 241-244.

Zhang, T., Li, L., Shang, Q., Lv, C., Wang, C., Su, B., 2015. Circulating miR-126 is a potential biomarker to predict the onset of type 2 diabetes mellitus in susceptible individuals. Biochem Biophys Res Commun 463, 60-63.

Zhang, T., Lv, C., Li, L., Chen, S., Liu, S., Wang, C., Su, B., 2013. Plasma miR-126 is a potential biomarker for early prediction of type 2 diabetes mellitus in susceptible individuals. Biomed Res Int 2013, 761617.

Supplementary Table 2. Comparison of $CD31^{+}$EV-shuttled miRNA relative expression among CTRL, T2DM-NC, and T2DM-C subjects. Variables are expressed as median (interquartile range). P value from Mann-Whitney *U* test for CTR vs. T2DM and from Kruskal-Wallis test for CTR vs. T2DM-NC vs. T2DM-C.

miRNA	**CTR**	**T2DM-C**	**T2DM-NC**	**p value (CTR vs. T2DM)**	**p value (CTR vs. T2DM-NC vs. T2DM-C)**
miR-126-3p	36.5 (44.4)	18.5 (21.0)	22.9 (34.7)	<0.001	<0.001
miR-146a-5p	0.4 (0.7)	1.7 (8.2)	30.8 (206.9)	<0.001	<0.001
miR-155	739.8 (677.1)	1.1 (1.2)	0.1 (0.9)	<0.001	<0.001
miR-195-5p	89.2 (60.4)	7.8 (7.1)	1.1 (7.9)	<0.001	<0.001
miR-21-5p	62.9 (100.4)	138.2 (127.5)	249.6 (156.8)	<0.001	<0.001
miR-24-3p	71.3 (109.2)	10.3 (8.8)	0.9 (6.1)	<0.001	<0.001
miR-320a	53.2 (110.9)	49.5 (83.5)	22.7 (37.9)	<0.001	<0.001
miR-342-3p	0.2 (0.2)	0.4 (0.5)	1.4 (2.5)	<0.001	<0.001
miR-376a	23.9 (146.9)	20.4 (46.2)	22.5 (150.6)	0.212	0.362
miR-422a	0.3 (0.6)	4.0 (7.4)	10.7 (8.2)	<0.001	<0.001
miR-451a	0.3 (0.3)	0.6 (0.7)	1.6 (1.5)	<0.001	<0.001

Supplementary Table 3. Binary logistic regression analysis of miRNAs associated with the presence of complications in T2DM patients. Odds ratio (95% CI) are expressed per 0.5 SD increase of each miRNA.

miRNA	**B**	**SE**	**P value**	**OR (95% CI)**
miR-146a-5p	0.693	0.343	0.043	1.999 (1.021 – 3.914)
miR-320a	-0.446	0.130	0.001	0.640 (0.496 – 0.826)
miR-422a	0.292	0.141	0.038	1.339 (1.016 – 1.763)
miR-451a	0.401	0.142	0.005	1.493 (1.131 – 1.973)

Supplementary Table 4. Binary logistic regression analysis of miRNAs associated with the presence of complications in T2DM patients. BMI and LDL-C were included into the model as covariates. Odds ratio (95% CI) are expressed per 0.5 SD increase of each miRNA.

miRNA	**B**	**SE**	**P value**	**OR (95% CI)**
miR-146a-5p	1.208	0.632	0.056	3.348 (0.969 – 11.563)
miR-320a	-0.874	0.268	0.001	0.417 (0.247 – 0.705)
miR-422a	0.616	0.304	0.043	1.852 (1.021 – 3.359)
miR-451a	0.804	0.304	0.008	2.235 (1.232 – 4.053)
BMI	-0.040	0.045	0.371	0.961 (0.880 – 1.049)
LDL-C	-0.015	0.006	0.023	0.986 (0.973 – 0.998)

Supplementary Table 5. Comparison of $CD31^+$-EV miRNA levels in T2DM individuals according to the presence of specific complications after adjustment for age and gender. In the case of MACE, comparisons after adjustment also for HbA1c and the presence of any other T2DM complication are also reported. P values of the comparison of the estimated marginal means are reported. Differences of the adjusted mean relative expressions between complication present and absent are reported where $p<0.05$.

miRNAs	At least one complication (n=101)	Neuropathy (n=28)	Nephropathy (n=20)	Retinopathy (n=48)	Peripheral artery disease (n=22)	MACE adj. for age and gender (n=52)	MACE adj. for age, gender, HbA1c, other complications (n=52)
miR-126-3p	0.214	0.166	0.693	0.309	0.312	0.213	0.949
miR-146a-5p	0.002 (125.6)	0.107	0.318	0.205	0.020 (124.5)	<0.001 (201.2)	<0.001 (204.8)
miR-155	<0.001 (-0.6)	0.192	0.980	0.542	0.013 (-0.45)	<0.001 (-1.1)	<0.001 (-1.0)
miR-195-5p	<0.001 (-5.3)	0.372	0.606	0.713	0.016 (-4.0)	<0.001 (-7.4)	0.002 (-5.7)
miR-21-5p	<0.001 (103.6)	0.903	0.538	0.522	0.970	<0.001 (131.2)	<0.001 (124.0)
miR-24-3p	<0.001 (-7.7)	0.168	0.175	0.497	0.008 (-4.8)	<0.001 (-9.8)	<0.001 (-7.3)
miR-320a	0.057	0.364	0.258	0.735	0.042 (-38.1)	0.065	0.962
miR-342-3p	<0.001 (1.2)	0.656	0.834	0.302	0.111	<0.001 (1.6)	<0.001 (1.5)
miR-376a	0.056	0.900	0.519	0.707	0.745	<0.001 (97.0)	<0.001 (92.6)
miR-422a	<0.001 (5.2)	0.685	0.737	0.517	0.064	<0.001 (6.2)	<0.001 (5.6)
miR-451a	<0.001 (0.8)	0.686	0.321	0.466	0.337	<0.001 (1.2)	<0.001 (1.3)

Supplementary Table 6. Complete correlation matrix of Pearson's correlations between 11 $CD31^{+}$EV miRNAs and selected clinical and biochemical variables.

Variables		miR-126-3p	miR-146a-5p	miR-155	miR-195-5p	miR-21-5p	miR-24-3p	miR-320a	miR-342-3p	miR-376a	miR-422a	miR-451a
Age	**r**	-0.026	0.149	-0.318	-0.415	0.252	-0.270	-0.084	0.224	0.039	0.301	0.281
	p	0.706	0.028	<0.001	<0.001	<0.001	<0.001	0.217	<0.001	0.567	<0.001	<0.001
BMI	**r**	0.007	0.096	-0.151	-0.176	0.138	-0.147	0.035	0.105	0.023	0.209	0.146
	p	0.920	0.160	0.026	0.009	0.043	0.030	0.603	0.121	0.733	0.002	0.032
Waist/hip ratio	**r**	-0.084	0.340	-0.217	-0.288	0.252	-0.224	-0.016	0.290	0.015	0.346	0.308
	p	0.217	<0.001	0.001	<0.001	<0.001	<0.001	0.813	<0.001	0.827	<0.001	<0.001
Fasting glucose	**r**	-0.162	0.163	-0.445	-0.513	0.281	-0.423	-0.170	0.272	-0.001	0.403	0.269
	p	0.017	0.016	<0.001	<0.001	<0.001	<0.001	0.012	<0.001	0.988	<0.001	<0.001
HbA1C	**r**	-0.086	0.173	-0.398	-0.475	0.271	-0.386	-0.122	0.295	0.055	0.382	0.286
	p	0.208	0.010	<0.001	<0.001	<0.001	<0.001	0.073	<0.001	0.418	<0.001	<0.001
Fasting insulin	**r**	-0.082	-0.012	-0.100	-0.095	0.012	-0.082	0.006	0.002	-0.021	-0.012	0.001
	p	0.229	0.855	0.140	0.162	0.858	0.225	0.929	0.976	0.756	0.860	0.985
HOMA index	**r**	-0.107	0.014	-0.176	-0.182	0.053	-0.157	-0.046	0.053	-0.022	0.056	0.046
	p	0.116	0.841	0.009	0.007	0.433	0.020	0.495	0.434	0.748	0.411	0.502
Azotemia	**r**	0.095	0.106	-0.100	-0.107	0.241	-0.101	0.153	0.280	0.126	0.152	0.390
	p	0.163	0.118	0.141	0.114	<0.001	0.136	0.024	<0.001	0.063	0.025	<0.001
Creatinine	**r**	0.078	0.206	-0.133	-0.197	0.310	-0.176	0.129	0.344	0.077	0.219	0.384
	p	0.250	0.002	0.049	0.003	<0.001	0.009	0.057	<0.001	0.257	0.001	<0.001
eGFR	**r**	-0.075	-0.119	0.080	0.138	-0.148	0.088	-0.003	-0.184	-0.088	-0.145	-0.198
	p	0.273	0.078	0.242	0.042	0.029	0.195	0.969	0.006	0.193	0.032	0.003
Uric acid	**r**	0.045	0.143	-0.060	-0.100	0.119	-0.081	-0.028	0.171	-0.005	0.107	0.082
	p	0.509	0.035	0.382	0.143	0.079	0.233	0.681	0.011	0.947	0.115	0.230
ALT	**r**	-0.054	0.016	-0.069	-0.051	-0.044	-0.052	0.013	0.043	-0.089	0.150	-0.098
	p	0.429	0.816	0.310	0.452	0.522	0.448	0.851	0.527	0.190	0.027	0.148
AST	**r**	-0.105	0.011	-0.075	-0.067	-0.004	-0.096	-0.060	0.050	-0.053	0.152	-0.064
	p	0.124	0.873	0.273	0.326	0.957	0.160	0.378	0.460	0.439	0.025	0.347
Gamma GT	**r**	-0.114	-0.007	-0.143	-0.149	0.046	-0.125	-0.150	0.126	-0.114	0.144	0.019
	p	0.094	0.919	0.034	0.028	0.498	0.065	0.027	0.063	0.092	0.034	0.778
Total bilirubin	**r**	-0.019	-0.036	0.071	0.097	-0.026	0.009	-0.054	0.016	-0.021	0.030	-0.023
	p	0.782	0.595	0.294	0.152	0.705	0.893	0.428	0.813	0.754	0.657	0.734

Variables		miR-126-3p	miR-146a-5p	miR-155	miR-195-5p	miR-21-5p	miR-24-3p	miR-320a	miR-342-3p	miR-376a	miR-422a	miR-451a
WBC	**r**	0.037	0.138	-0.088	-0.162	0.127	-0.153	-0.114	0.205	0.001	0.165	0.155
	p	0.586	0.042	0.196	0.017	0.061	0.023	0.094	0.002	0.983	0.015	0.022
RBC	**r**	-0.066	0.056	-0.181	-0.169	0.053	-0.199	-0.163	0.019	0.032	0.117	0.048
	p	0.334	0.414	0.007	0.012	0.432	0.003	0.016	0.783	0.638	0.085	0.478
Hemoglobin	**r**	-0.103	0.034	-0.165	-0.167	0.078	-0.173	-0.123	0.026	-0.001	0.095	0.011
	p	0.129	0.619	0.015	0.013	0.254	0.010	0.070	0.704	0.989	0.162	0.869
Hematocrit	**r**	-0.082	0.064	-0.177	-0.191	0.063	-0.182	-0.117	0.040	0.014	0.106	0.032
	p	0.226	0.344	0.009	0.005	0.352	0.007	0.084	0.552	0.842	0.119	0.643
Serum iron	**r**	-0.086	-0.062	-0.025	-0.017	0.021	-0.029	-0.157	0.023	-0.030	0.022	-0.050
	p	0.206	0.363	0.714	0.803	0.753	0.667	0.020	0.736	0.661	0.750	0.467
Transferrin	**r**	-0.106	0.012	-0.134	-0.091	0.047	-0.007	0.011	0.089	-0.095	0.084	0.055
	p	0.119	0.862	0.048	0.182	0.490	0.915	0.875	0.192	0.163	0.218	0.419
Ferritin	**r**	-0.086	-0.025	-0.007	-0.014	0.039	-0.094	-0.080	0.115	-0.078	0.073	-0.031
	p	0.204	0.715	0.923	0.837	0.569	0.168	0.238	0.091	0.254	0.282	0.653
Platelets	**r**	0.028	-0.028	0.096	0.087	-0.146	0.121	0.021	-0.121	-0.077	-0.081	-0.065
	p	0.684	0.681	0.159	0.199	0.031	0.074	0.754	0.074	0.255	0.234	0.342
Total cholesterol	**r**	0.109	-0.197	0.109	0.159	-0.175	0.171	-0.005	-0.214	-0.115	-0.239	-0.210
	p	0.108	0.003	0.110	0.019	0.010	0.012	0.943	0.001	0.090	<0.001	0.002
HDL-cholesterol	**r**	0.036	-0.181	0.247	0.314	-0.273	0.299	0.052	-0.243	-0.058	-0.343	-0.250
	p	0.596	0.007	<0.001	<0.001	<0.001	<0.001	0.444	<0.001	0.395	<0.001	<0.001
LDL-cholesterol	**r**	0.066	-0.235	0.104	0.168	-0.162	0.169	-0.010	-0.269	-0.054	-0.247	-0.222
	p	0.334	<0.001	0.126	0.013	0.017	0.012	0.888	<0.001	0.432	<0.001	<0.001
ApoA1	**r**	0.056	-0.175	0.197	0.296	-0.234	0.293	0.033	-0.203	-0.014	-0.319	-0.202
	p	0.408	0.009	0.003	<0.001	<0.001	<0.001	0.626	0.003	0.832	<0.001	0.003
ApoB	**r**	0.119	-0.124	0.078	0.156	-0.074	0.131	0.015	-0.161	-0.016	-0.190	-0.108
	p	0.080	0.068	0.254	0.021	0.278	0.054	0.826	0.017	0.812	0.005	0.112
Triglycerides	**r**	-0.016	0.109	-0.112	-0.127	0.051	-0.114	-0.028	0.156	-0.096	0.162	0.049
	p	0.809	0.110	0.099	0.062	0.452	0.092	0.678	0.021	0.156	0.017	0.471
hs-CRP	**r**	-0.044	0.180	-0.085	-0.115	0.055	-0.094	-0.039	0.131	0.059	0.141	0.009
	p	0.515	0.688	0.213	0.089	0.422	0.165	0.567	0.054	0.383	0.038	0.895
Fibrinogen	**r**	0.152	0.070	-0.057	-0.086	0.129	-0.097	0.047	0.208	-0.032	0.206	0.228
	p	0.034	0.329	0.426	0.230	0.072	0.177	0.510	0.004	0.652	0.004	0.001

Variables		miR-126-3p	miR-146a-5p	miR-155	miR-195-5p	miR-21-5p	miR-24-3p	miR-320a	miR-342-3p	miR-376a	miR-422a	miR-451a
PAI-1	**r**	-0.057	0.022	-0.088	-0.138	-0.071	-0.086	-0.028	-0.010	-0.066	-0.008	-0.043
	p	0.404	0.744	0.194	0.041	0.299	0.207	0.681	0.889	0.334	0.901	0.532
Total proteins	**r**	-0.052	0.034	-0.130	-0.162	0.077	-0.167	-0.132	0.179	-0.048	0.273	0.107
	p	0.441	0.620	0.056	0.017	0.260	0.013	0.051	0.008	0.480	<0.001	0.115
Telomere length	**r**	-0.021	-0.221	0.123	0.154	-0.185	0.111	0.005	-0.295	-0.031	-0.216	-0.200
	p	0.755	0.001	0.073	0.025	0.007	0.106	0.948	<0.001	0.651	0.002	0.003
miR-126-3p	**r**	1.000	0.098	0.222	0.313	0.079	0.143	0.169	0.110	-0.053	-0.016	0.143
	p	NA	0.148	<0.001	<0.001	0.244	0.035	0.012	0.104	0.434	0.811	0.035
miR-146a-5p	**r**	0.098	1.000	-0.173	-0.221	0.330	-0.211	0.065	0.590	0.054	0.440	0.405
	p	0.148	NA	0.010	0.001	<0.001	0.002	0.342	<0.001	0.429	<0.001	<0.001
miR-155	**r**	0.222	-0.173	1.000	0.832	-0.437	0.792	0.153	-0.314	0.055	-0.439	-0.331
	p	<0.001	0.010	NA	<0.001	<0.001	<0.001	0.023	<0.001	0.417	<0.001	<0.001
miR-195-5p	**r**	0.313	-0.221	0.832	1.000	-0.488	0.752	0.253	-0.393	0.056	-0.539	-0.394
	p	<0.001	0.001	<0.001	NA	<0.001	<0.001	<0.001	<0.001	0.409	<0.001	<0.001
miR-21-5p	**r**	0.079	0.330	-0.437	-0.488	1.000	-0.419	-0.007	0.686	0.055	0.723	0.686
	p	0.244	<0.001	<0.001	<0.001	NA	<0.001	0.913	<0.001	0.417	<0.001	<0.001
miR-24-3p	**r**	0.143	-0.211	0.792	0.752	-0.419	1.000	0.232	-0.353	0.034	-0.479	-0.355
	p	0.035	0.002	<0.001	<0.001	<0.001	NA	<0.001	<0.001	0.615	<0.001	<0.001
miR-320a	**r**	0.169	0.065	0.153	0.253	-0.007	0.232	1.000	0.027	-0.056	-0.140	0.136
	p	0.012	0.342	0.023	<0.001	0.913	<0.001	NA	0.696	0.409	0.039	0.044
miR-342-3p	**r**	0.110	0.590	-0.314	-0.393	0.686	-0.353	0.027	1.000	0.015	0.741	0.720
	p	0.104	<0.001	<0.001	<0.001	<0.001	<0.001	0.696	NA	0.825	<0.001	<0.001
miR-376a	**r**	-0.053	0.054	0.055	0.056	0.055	0.034	-0.056	0.015	1.000	0.068	0.073
	p	0.434	0.429	0.417	0.409	0.417	0.615	0.409	0.825	NA	0.320	0.282
miR-422a	**r**	-0.016	0.440	-0.439	-0.539	0.723	-0.479	-0.140	0.741	0.068	1.000	0.632
	p	0.811	<0.001	<0.001	<0.001	<0.001	<0.001	0.039	<0.001	0.320	NA	<0.001
miR-451a	**r**	0.143	0.405	-0.331	-0.394	0.686	-0.355	0.136	0.720	0.073	0.632	1.000
	p	0.035	<0.001	<0.001	<0.001	<0.001	<0.001	0.044	<0.001	0.282	<0.001	NA